NASA TECHNICAL NOTE

NASA TN D-6410

DETERMINATION OF PRIMARY-ZONE SMOKE CONCENTRATIONS FROM SPECTRAL RADIANCE MEASUREMENTS IN GAS TURBINE COMBUSTORS

by Carl T. Norgren

Lewis Research Center
Cleveland, Ohio 44135

NATIONAL AERONAUTICS AND SPACE ADMINISTRATION • WASHINGTON, D. C. • JULY 1971

1. Report No.	2. Government Accession No.	3. Recipient's Catalog No.
NASA TN D-6410		

4. Title and Subtitle	5. Report Date
DETERMINATION OF PRIMARY-ZONE SMOKE CONCENTRATIONS FROM SPECTRAL RADIANCE MEASUREMENTS IN GAS TURBINE COMBUSTORS	July 1971
	6. Performing Organization Code
7. Author(s)	8. Performing Organization Report No.
Carl T. Norgren	E-6083
	10. Work Unit No.
9. Performing Organization Name and Address	720-03
Lewis Research Center National Aeronautics and Space Administration Cleveland, Ohio 44135	11. Contract or Grant No.
	13. Type of Report and Period Covered
12. Sponsoring Agency Name and Address	Technical Note
National Aeronautics and Space Administration Washington, D.C. 20546	14. Sponsoring Agency Code

15. Supplementary Notes

16. Abstract

The smoke concentration within the primary zone of an experimental combustor operating at pressures up to 20 atmospheres was determined with a technique using spectral radiance measurements. Exhaust smoke concentration was obtained from reflectance readings of stained filter paper. The primary zone smoke concentration was of the order of 100 to 1000 times greater than at the exhaust. The smoke oxidation rate obtained is compared with reported values for coal particles and seeded laboratory flames. Primary zone smoke concentration was shown to be related to exhaust smoke number and total radiance.

17. Key Words (Suggested by Author(s))	18. Distribution Statement
	Unclassified - unlimited

19. Security Classif. (of this report)	20. Security Classif. (of this page)	21. No. of Pages	22. Price*
Unclassified	Unclassified	47	$3.00

*For sale by the National Technical Information Service, Springfield, Virginia 22151

DETERMINATION OF PRIMARY-ZONE SMOKE CONCENTRATIONS FROM SPECTRAL RADIANCE MEASUREMENTS IN GAS TURBINE COMBUSTORS

by Carl T. Norgren

Lewis Research Center

SUMMARY

The smoke concentration within the primary zone of an experimental combustor operating at total pressure of 10 and 20 atmospheres was determined with a technique using spectral radiance measurements. The exhaust smoke concentration was based on correlations relating concentration to smoke number values as obtained from reflectance readings of stained filter paper tape. The primary zone smoke concentration was of the order of 100 to 1000 times greater than at the exhaust. The smoke oxidation rate of 2.5×10^{-4} grams of carbon per square centimeter per second is compared with reported values for coal particles and seeded laboratory flames.

The emittance of the incandescent smoke formed in the primary zone was the major contributor to the total measured radiance; that is, it was much greater than the spectral radiance of the combustion products, water vapor and carbon dioxide. The relation between exhaust smoke number and total radiance was established. Major improvements in lowering the total flame radiation are shown to be possible by a reduction in exhaust smoke level. All the combustor designs investigated incorporated features that improved the mixing of the primary fuel and air. It was demonstrated that at the most severe operating condition of 20 atmospheres pressure and inlet temperature of 589 K (1060° R) a smoke number level of 4 could be achieved. This same combustor showed a threefold reduction in the total radiance to the combustor walls for a take-off condition as compared with a combustor operating at a smoke level of 32 (visible threshold 20 to 30).

INTRODUCTION

The Lewis Research Center is engaged in programs directed towards improving the performance of turbojet engine combustors. As part of this program a study was undertaken to evaluate the smoke produced by the combustion of hydrocarbon fuels during simulated takeoff conditions in a high-bypass-ratio turbofan engine with a 20 to 1 compression ratio.

Smoke is objectionable at the combustor exhaust because it is emitted into the atmosphere in the jet exhaust thereby causing an unsightly smoke trail as well as polluting the atmosphere. Smoke is also objectionable in the combustor because it is responsible for excessive radiant heat transfer to the combustor liner walls thus compounding liner cooling and durability problems. The mechanisms whereby smoke is formed within the combustor are not clearly defined; however, fuel type, hydrogen-carbon ratio, fuel preparation, including atomization and vaporization, and the mixing of the fuel with combustion air has a pronounced effect on the smoking tendency of a combustor. Combustor operating parameters of inlet temperature, pressure, and reference velocity also affect smoking tendency. The most severe smoking problem occurs when the combustor is operated at high compressor pressure levels and the local fuel-air ratio is above the threshold of smoke formation as discussed in references 1 and 2.

To study methods of reducing smoke formation and to determine smoking tendency, it is desirable to be able to quantitatively determine smoke concentration. Until recently there have been no satisfactory methods of determining smoke in the combustor primary flame zone. Attempts have been made to physically sample the flame, however, as combustor pressure and temperature are increased sampling becomes increasingly more difficult as discussed in reference 3. It is the purpose of this report to demonstrate a technique whereby (1) the smoke concentrations produced in the primary zone of a combustor can be determined optically, (2) the smoke remaining at the combustor exhaust can be determined from the smoke number, and (3) the reaction rate associated with the smoke oxidation calculated. The technique will enable the designer to study smoke formation within the combustor on a quantitative basis rather than from the limited data, which can be inferred from exhaust smoke measurements. To accomplish this goal it is necessary to take advantage of recent developments in various related fields.

The concentration of smoke within large furnace flames at atmospheric pressure has been correlated with respect to flame emissivity by numerous investigators as reported in references 4 to 7. These investigations were based on the premise that once the spectral flame emissivity is known, the concentration of the smoke can be calculated from a knowledge of the path length and the spectral absorption coefficient. It has been shown that the classical small particle radiation theory, as proposed by Mie,

is applicable in predicting the spectral absorption coefficient of carbon smoke as discussed in references 8 to 11. Emissivity can be obtained from the actual flame radiance and the blackbody flame temperature.

The emissivity of the high pressure flame can also be determined optically. The technique described in this report offers the major advantage of being able to determine the primary zone smoke concentration by means of an optical measurement for high pressure combustion rather than to cope with the formidable problems involved in sampling. In application to the combustor smoke problem, the flame radiance can be experimentally obtained at a wavelength where the hot combustion gases are transparent and the observed radiance is due only to smoke. The flame temperature can be obtained in a spectral region where the hot combustion gases can be considered as a blackbody radiator as discussed in references 12 to 16. Therefore, by selection of proper wavelength intervals combustor smoke concentrations can be readily calculated.

The smoke concentration at the combustor exhaust can be determined by sampling, since the environment is considerably less severe than in the primary combustion zone. A gravimetric determination of the smoke is difficult due to the relatively small quantity of carbon entrained. In practice, the degree of smoking is obtained by passing a fixed volume of exhaust gas through a given area of filter paper. A smoke number determined in this manner can then be correlated to the mass concentration of carbon as presented in references 17 and 18.

The oxidation of carbon particles has been extensively investigated with respect to pulverized coal as reported in references 19 to 22. Recent studies have centered on the reaction as simulated by seeding a laboratory flame with soot (refs. 23 and 24). The carbon particle oxidation rate is then determined from the differences in the initial and final mass concentrations and residence time. In the present study a similar model was assumed to calculate the specific reaction rate of the smoke burnup within the high pressure turbojet combustor.

The experimental combustors were designed to produce a low smoke number in a short length while operating at pressure levels to 20 atmospheres. The approach was based on the establishment of a lean primary zone coupled with intense mixing of atomized fuel and air to prevent local overrich zones. Data were obtained to determine (1) the concentration level of smoke produced in the primary combustion zone, (2) the concentration of smoke at the combustor exhaust, (3) the rate of smoke oxidation within the combustor, and (4) the total radiance from the combustion products in the primary combustion zone.

ANALYTICAL TECHNIQUE

This section of the report will describe the methods used to determine (1) primary zone smoke concentration, (2) smoke concentration at the combustor exhaust, (3) smoke oxidation rate within the combustor, and (4) total radiance in the primary zone. The symbols used in the equations are defined in appendix A. For convenience carbon formed during combustion will be referred to as smoke whether existing as an aerosol or deposit.

Primary Zone Smoke Concentration

The smoke concentration within a radiating cloud can be related to its emissivity by means of Beér's Law:

$$\epsilon_\lambda = 1 - \exp\left(c l K_{T,\lambda}\right) \tag{1}$$

where ϵ_λ is the spectral emissivity of the smoke, $K_{T,\lambda}$ the total extinction coefficient, c the concentration of the smoke, and l the optical path length. All measurements and values refer to a single wavelength λ. In order to determine the concentration of the smoke, it is more convenient to express equation (1) in the form

$$c = \frac{-\ln\left(1 - \epsilon_\lambda\right)}{l K_{T,\lambda}} \tag{1b}$$

To calculate the smoke concentration, it is necessary to experimentally evaluate the spectral emissivity ϵ_λ of the smoke and to assign an appropriate value to the extinction coefficient $K_{T,\lambda}$.

Considerations in the evaluation of the spectral emissivity of the smoke. - The spectral emissivity of the smoke for a given wavelength λ is defined as

$$\epsilon_\lambda = \frac{L_\lambda}{L_{B,\lambda}} \tag{2}$$

where L_λ is the spectral radiance of the smoke and $L_{B,\lambda}$ is the blackbody spectral radiance evaluated at the temperature of the smoke.

The following assumptions were made in the determination of the smoke emissivity from equation (2):

(1) The spectral radiance of the smoke can be measured in a flame over a wavelength interval where the radiation from the combustion products (water vapor and carbon dioxide) are transparent.

(2) The temperature of the combustion products can be determined over a wavelength interval where their emissivity can be assumed as unity.

(3) The smoke is in thermodynamic equilibrium with the surrounding combustion products.

(4) The combustion products can be represented by a single value of temperature.

In order to select the two wavelength intervals required to determine the spectral emissivity of the smoke, it is necessary to consider the radiant characteristics of the combustion products.

The smoke radiates over a continuum spectrum as shown in references 8 to 11. The attenuation of radiation is described in terms of an extinction coefficient. The total extinction coefficient $K_{T,\lambda}$ is equal to the fraction absorbed plus that scattered. That is,

$$K_{T,\lambda} = K_{\lambda} + K_{s,\lambda} \tag{3}$$

Scattering contributes significantly only when particle size and wavelength are of the same magnitude. It has been shown in references 4 and 13 that smoke particles formed within the flame zone average less than 0.06 micrometer in diameter, so that, if measurements are made only at wavelengths greater than 1 micrometer, extinction due to scattering may be neglected compared with that due to absorption (see ref. 10).

The gaseous products of combustion, water vapor, and carbon dioxide, emit radiation in a different manner. Gases differ in their behavior from solid bodies insofar as they absorb and emit radiation only within discrete wavelengths. The predominant emission bands of water vapor associated with the infrared band spectra up to 6 micrometers are centered normally at 1.38, 1.87, 2.7, 3.2, and 5.7 micrometers. Similarly, the predominate emission bands for carbon dioxide are 2.0, 2.7, 4.3, 4.8, and 5.2 micrometers as tabulated from reference 25.

From these considerations of the radiating species, two narrow-band interference filters were selected to measure the two required spectral radiances: (1) a narrow-band interference filter peaking at 4.05 micrometers to detect the spectral radiance in the continuum spectra of the smoke without interference from water vapor or carbon dioxide and (2) a narrow band interference filter peaking at 2.70 micrometers to determine the flame blackbody temperature from the major radiating band of water vapor.

In order to determine the flame temperature from absorption spectra, it is required that all radiating species must be at the same temperature. Under these conditions, Kirchoff's law applies, and absorption equals radiance. Reference 13 showed

that the smoke could be assumed to be at the same temperature as its surroundings; therefore, the determination of the flame temperature was also considered as representative of the temperature of the smoke. To correctly evaluate the true flame temperature it is necessary to consider the design features of the experimental combustors.

The principle objective of the experimental combustor configuration was to provide a lean primary zone to prevent over rich fuel pockets from forming, and hence, to reduce smoke formation. This feature was accomplished in a unique manner which enabled all the air required for complete combustion of the fuel to be introduced through swirlers concentric to the fuel nozzles. The intense mixing region established in the resultant vortex promoted a more uniform temperature distribution than would otherwise be obtained in a conventional combustor configuration. In addition, by limiting the field of view, gradients within the flame can be further minimized. Under these conditions it was assumed that a single value of measured flame temperature was characteristic of the radiating combustion products.

Calculation of the emissivity of the smoke. - The spectral emissivity of the smoke is calculated from equation (2). Measurements taken at 4.05 micrometers represent the actual spectral radiance L_λ of the smoke. It is necessary to compare spectral radiances L_λ and $L_{B,\lambda}$ at the same wavelength in order to calculate the emissivity of the smoke. Therefore, $L_{B,\lambda}$ must be determined by first determining the blackbody temperature of the flame. The spectral radiance measurement at 2.70 micrometers was used to calculate the blackbody flame temperature. The radiometer output in millivolts was proportional to the incident spectral radiation. It was not possible to obtain an absolute value of L_λ. In actual practice the radiometer calibration curves provided two equivalent blackbody temperatures: a temperature T representative of the continuum spectra of the smoke ($\lambda = 4.05\ \mu m$) and a blackbody temperature of the flame T_B ($\lambda = 2.70\ \mu m$). The blackbody spectral radiance at 4.05 micrometers was therefore calculated in the following manner: Spectral blackbody radiance is related to wavelength and temperatures by Planck's equation as follows:

$$L_\lambda = \frac{c_1}{\lambda^5}\left[\frac{1}{\exp\left(\frac{c_2}{\lambda T}\right) - 1}\right] \tag{4}$$

where L_λ is the spectral blackbody radiance at a wavelength of λ and c_1 and c_2 are constants. The term L_λ can be expressed as a function of T by dividing each side of equation (4) by T^5.

$$\frac{L_\lambda}{T^5} = \frac{c_1}{(\lambda T)^5}\left[\frac{1}{\exp\left(\frac{c_2}{\lambda T - 1}\right)}\right] \tag{5}$$

The value of L_λ is obtained by the following integration over the wavelength of interest for the spectral radiance of the smoke:

$$L_\lambda = \int_{\lambda_1=4.015}^{\lambda_2=4.085} L_\lambda d\lambda \tag{6}$$

Equation (6) can be rewritten using equation (5) and integrating over a range of λT:

$$L_\lambda = \delta T^4 \int_{\lambda_1 T}^{\lambda_2 T} \frac{L_\lambda}{\delta T^5} d(\lambda T) = \delta T^4 \int_{\lambda_1 T}^{\lambda_2 T} \frac{c_1}{\delta(\lambda T)^5}\left[\frac{1}{\exp\frac{c_2}{\lambda T - 1}}\right] d(\lambda T) \tag{7}$$

The spectral radiance L_λ may be calculated from equation (7) with λ_1, λ_2, and T known and using a Planck radiation-function table which lists

$$\int_0^{\lambda T} \frac{L_\lambda}{\delta T^5} d(\lambda T)$$

as a function of λT. The spectral radiance L_λ obtained in this manner (from the equivalent blackbody temperature T provided by the radiometer calibration curve at $\lambda = 4.05$ μm) represents the actual spectral radiance from the smoke over this bandwidth region without attenuation. The computation was repeated to obtain $L_{B,\lambda}$ using T_B provided by the radiometer calibration curve at $\lambda = 2.7$ micrometers and integrated over the same wavelength interval. The calculated values of L_λ and $L_{B,\lambda}$ were substituted into equation (2) to obtain the emissivity of the smoke.

Determination of the extinction coefficient $K_{T,\lambda}$. - The total extinction coefficient is equal to the fraction of radiation absorbed plus that scattered as defined in equation (3). Since measurements are made at 4.05 micrometers, the scattering coefficient can be neglected as previously discussed. A numerical value of the absorption coefficient

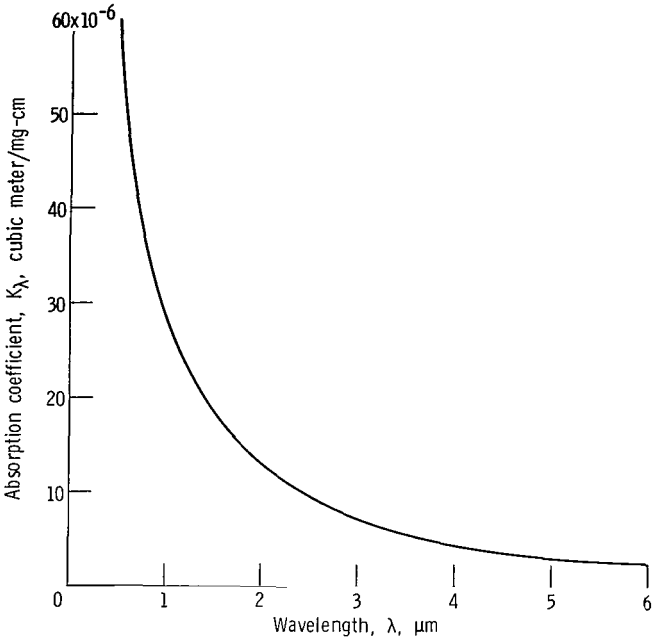

Figure 1. - Specific absorption coefficient of cloud of carbon particles calculated using Mie theory for carbon electrode (ref. 10).

characteristic of carbon graphite was selected from the theoretical value reported by Foster in reference 10. A plot of this theoretical value is shown in figure 1 for a wavelength band from 0.5 to 6.0 micrometers. The value of the absorption coefficient at a wavelength of 4.05 micrometers is 4.3×10^{-6} cubic meter per milligram per centimeter.

The following additional factors were considered in the selection of the value of the absorption coefficient:

(1) The experimentally determined values of spectral emittance of thin layers of soot were compared with values calculated from the Foster solution of the Mie theory in reference 26. The agreement between the experiment and theory was good suggesting that the Foster solution to the Mie theory can be used to determine smoke concentrations in a gas turbine combustor from radiation measurements.

(2) The absorption coefficient is independent of temperature; therefore, temperature gradients within the flame need not be considered.

(3) The absorption coefficient is independent of particle size distribution.

(4) The absorption coefficient is dependent on the composition of the smoke particle as discussed in references 9 and 27. It was assumed that a single value for the absorption coefficient could be used in this study since only one type of fuel was used.

Calculation of the primary zone smoke concentration. - The smoke concentration was calculated from equation (1b). The smoke spectral emissivity, the absorption coefficient, and an optical path length equal to the combustor width of 30.48 centimeters (12 in.) were substituted into equation (1b). The concentration of smoke particles is not

necessarily uniform along the viewing path. The product, however, is equivalent to a direct summation of the smoke population so that the result is also applicable in a non-uniform situation as noted in reference 5.

Smoke Concentration at the Combustor Exhaust

A recent standard has been established by the Society of Automotive Engineers (SAE) to evaluate the amount of smoke produced by jet engines (ref. 28). In this method a Whatman No. 4 filter paper is stained by a known volume of airborne smoke. The resulting stained filter paper is analyzed against a black background by means of a reflectance densitometer. The reflectance reading of the sample is compared with that of the clean filter material and a smoke number rating established as defined by the equation:

$$\text{Smoke Number} = 100\left[1 - \frac{R_s}{R_w}\right] \tag{8}$$

Several investigators have attempted to correlate the smoke number to the actual concentration of smoke in the sample as reported in references 18 and 29. Correlated

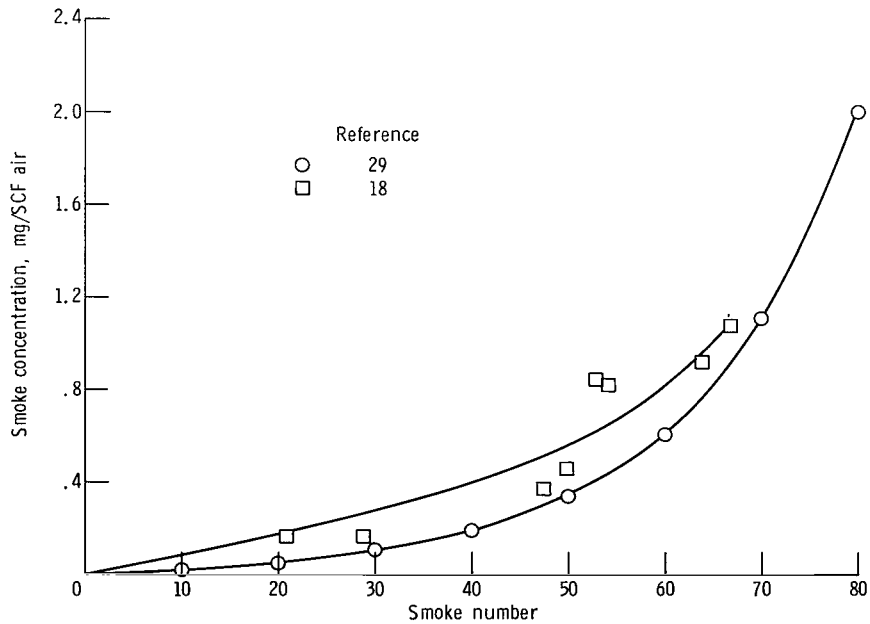

Figure 2. - Exhaust smoke concentration associated with smoke number.

smoke concentration with smoke number from these references is shown in figure 2. The data of reference 29 were obtained by installing a small centrifugal filter in the sampling line, since it was believed that the observed scatter in that data was due to agglomerated carbon particles. As a possible result of the elimination of the larger particles, the data of reference 29 appear low. Since all the smoke sample was passed through the filter paper without regard to particle agglomeration, it was elected in this report to use the correlation as representative from reference 18 to correlate smoke number to carbon smoke concentration.

Smoke Oxidation Rate Within the Combustor

The smoke oxidation rate was calculated from the difference in smoke concentration determined in the primary zone and at the combustor exhaust. The rate of change of mass with time can be expressed in terms of the reaction rate as shown in reference 23 as

$$R = \frac{\rho d_0}{6\, c_0^{1/3}\, c^{1/3}} \frac{dc}{dt} \tag{9}$$

where R is the specific reaction rate, d the particle diameter, and c the mass concentration. The subscript 0 refers to an arbitrary initial state. In order to apply equation (9), it is necessary to assume that (1) the initial size of the particles can be represented by a uniform average diameter, (2) the number of particles in the system remains constant, and (3) the size of the smoke particles decreases as the particles undergo oxidation.

The specific reaction rate obtained from the integrated form of equation (9) is

$$R = \frac{\rho d_0}{2t}\left(1 - \left(\frac{c}{c_0}\right)^{1/3}\right) \tag{10}$$

The initial and final smoke concentrations were obtained as previously described. It was assumed that the dilution air quenched the reaction. The residence time t for the reaction was assumed to be proportional to the reaction zone length and inversely proportional to the combustor reference velocity

$$t = \frac{l'}{V_R} \tag{11}$$

The choice of the initial particle diameter is arbitrary. Initial particle diameters have been reported in the range of 0.5 to 6×10^{-6} centimeter. The initial diameter of the particle was taken as 1×10^{-6} centimeter, which is similar to the value reported and correlated in reference 24. The particle density was assumed to be about equal to the bulk density of carbon (2.00 g/cm^3). It should be noted that the value of particle density is arbitrary because of the manner in which the individual atoms are arranged and because of the differences in packing density as reported in reference 30.

Total Radiance in the Primary Zone

The total radiance L was calculated from the partial radiance of the flame measured over a band range from 0.25 to 6.0 micrometers. The blackbody temperature of the combustion products and smoke was obtained in the manner previously discussed from the radiometer calibration curves. This temperature was used to calculate the blackbody radiance using the Stephan-Boltzmann equation

$$L = \epsilon\sigma T^4 \tag{12}$$

A blackbody total radiance was calculated using the blackbody flame temperature determined from the 2.7-micrometer band-pass filter measurement. Total flame emissivity was calculated from the two values of radiance using the equation

$$\epsilon_T = \frac{L}{L_B} \frac{(T \text{ determined from } \lambda = 0.25 \text{ to } 6.0)}{(T \text{ determined at } \lambda = 2.7)} \tag{13}$$

EXPERIMENTAL APPARATUS AND PROCEDURE

Test Duct and Combustors

A schematic of the experimental test rig is shown in figure 3. Inlet air pressures up to 27 atmospheres can be supplied at temperature to 589 K (1060° R) with the indirect fired preheater and up to 922 K (1660° R) with vitiation. A cylindrical pressure shell is used to contain the relatively lightweight rectangular combustor housing, and a counterflow air passage is provided to supply a continuous flow of air around the housing within the pressure shell. Short tubes connect the passages between the outside housing and the inner combustor side walls. These tubes terminate in a well in which two sapphire windows are mounted in tandem for each position. Nitrogen impinges on the inner sur-

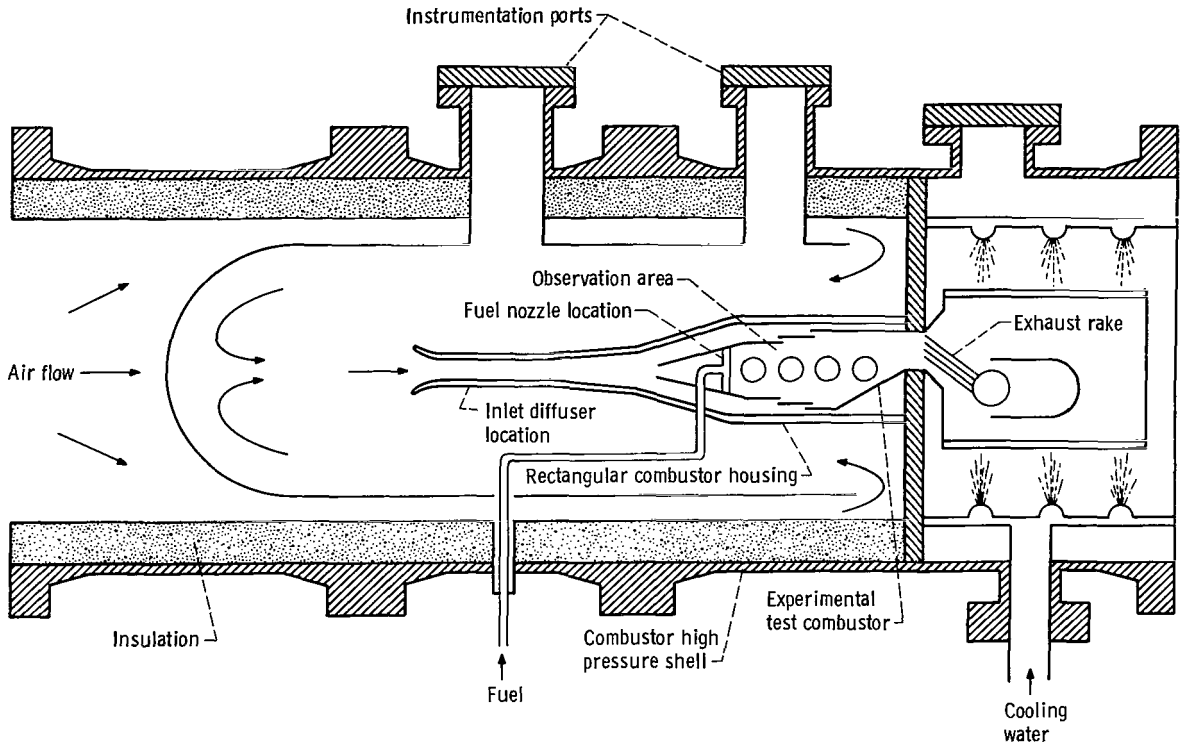

Figure 3. - Experimental test rig.

face of the windows to keep them clean. The well is pressurized slightly (of the order of 2.54 cm (1 in.) of mercury) above the combustor operating pressure.

Combustors featuring high intensity mixing of the primary air and fuel were designed to reduce smoke formation and to provide a desired short-length combustor configuration as discussed in reference 31. The 31.75-centimeter (12.5 in.) combustors (from fuel nozzle to exhaust plane) were installed in the test housing, which has a rectangular cross section of 15.24 by 30.46 centimeters (6 by 12 in.). The primary combustion zone was 15.24 centimeters (6 in.) long. Primary air was admitted through swirlers which provided varying degrees of vorticity for primary airflows which range from 14 to 34 percent of the total airflow. The dilution mixing zone was patterned after the dilution zone reported in reference 32 and had an overall length of 16.50 centimeters (6.5 in.). For these tests, three combustor configurations were selected to demonstrate smoke formation: (1) combustor model A which had the highest level of exhaust smoke, (2) combustor model B which had the lowest smoke level, and (3) combustor model C which had a higher smoke level than combustor B but would be more satisfactory for engine application because of outlet temperature profile considerations. Details of the combustor configurations are presented in appendix B for the three combustor models.

Additional data from other combustor configurations are included to evaluate trends of specific reaction rate, total radiation, and smoke number.

Radiometric System and Calibration

The radiometric equipment incorporated a high-sensitivity detector for low-level spectral radiance measurements, and also a bolometer detector to measure total radiance. The dual system, including detectors, beam splitters, and filters, was assembled using commercially available components by Barnes Engineering Company under NASA contract. A photograph of the unit is shown in figure 4. The radiometer was selected because of its ability to provide relatively high signal strength with small target area and narrow band interference filters in the optical path. The instrument was remotely controlled and capable of withstanding the test cell environment. The small target area was desired to minimize flame profile temperature gradients, to keep the observation windows small, and to simplify auxilliary blackbody furnace requirements for calibra-

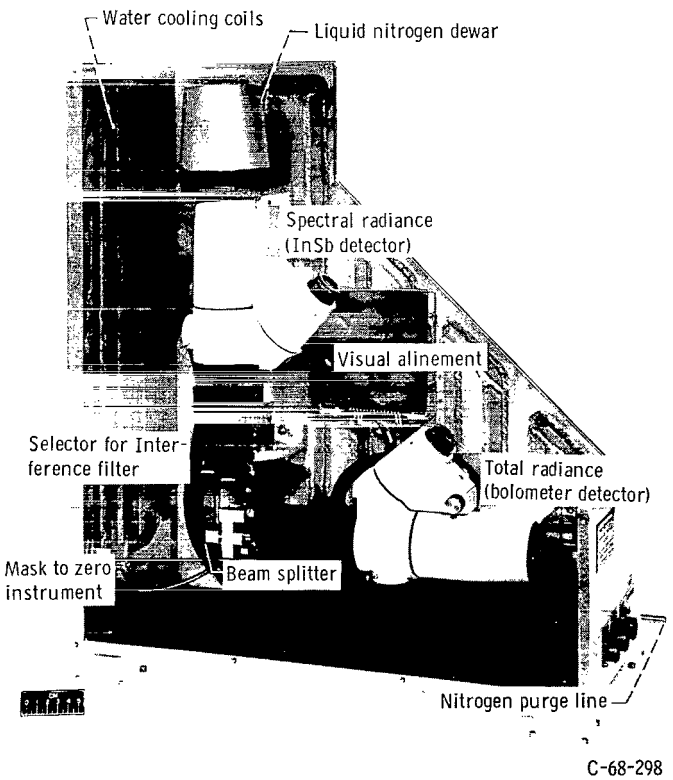

Figure 4. - Photograph of assembled radiometric unit.

tion. The radiometers were positioned so that the fields of view coincided at the blackbody reference furnace.

Spectral radiance radiometer. - A commercially available infrared radiometric microscope, using an indium antimonide detector with a sensitivity range from 1 to 5.8 micrometers at 77 K, was used. The unit was modified by changing the lens system so that a small spot source 0.64 centimeter (0.25 in.) in diameter could be focused onto the detector from a distance of 1.80 meter (71 in.). A schematic of the radiometer head is shown in figure 5. The head contains the optics, a detector, a preamplifier, a chopper, a visual sighting channel, and a liquid-nitrogen flask to cool the detector. The tuning fork chopper modulates the incoming radiation to the detector thereby producing an alternating voltage at the input to the signal processing electronics. A remote-control unit contains the electronics for the chopper and signal processing.

Total radiance bolometer. - A commercially available radiometric microscope using an unimmersed bolometer thermal detector with a sensitivity range from 0.25 to 6 micrometers was modified by changing the lens system so that a small spot 0.32 centimeter (0.125 in.) in diameter could be focused from a distance of 1.80 meter (71 in.) onto the detector. The radiometer was similar to the indium antimonide detector without the dewar and was made up the other half of the dual radiometer. The signal was chopped at a different frequency and an extra preamplifier stage was added for the total radiance bolometer. A smaller target area was obtained with a less sensitive detector (bolometer) because of the broad spectral range.

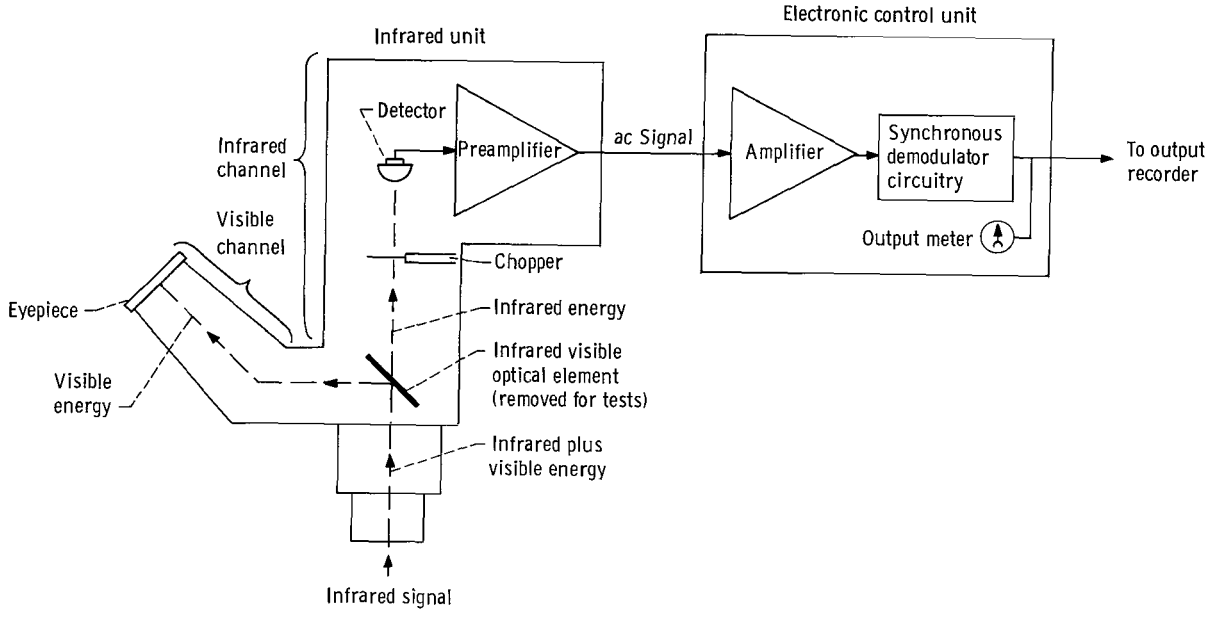

Figure 5. - Schematic of typical infrared radiometric unit.

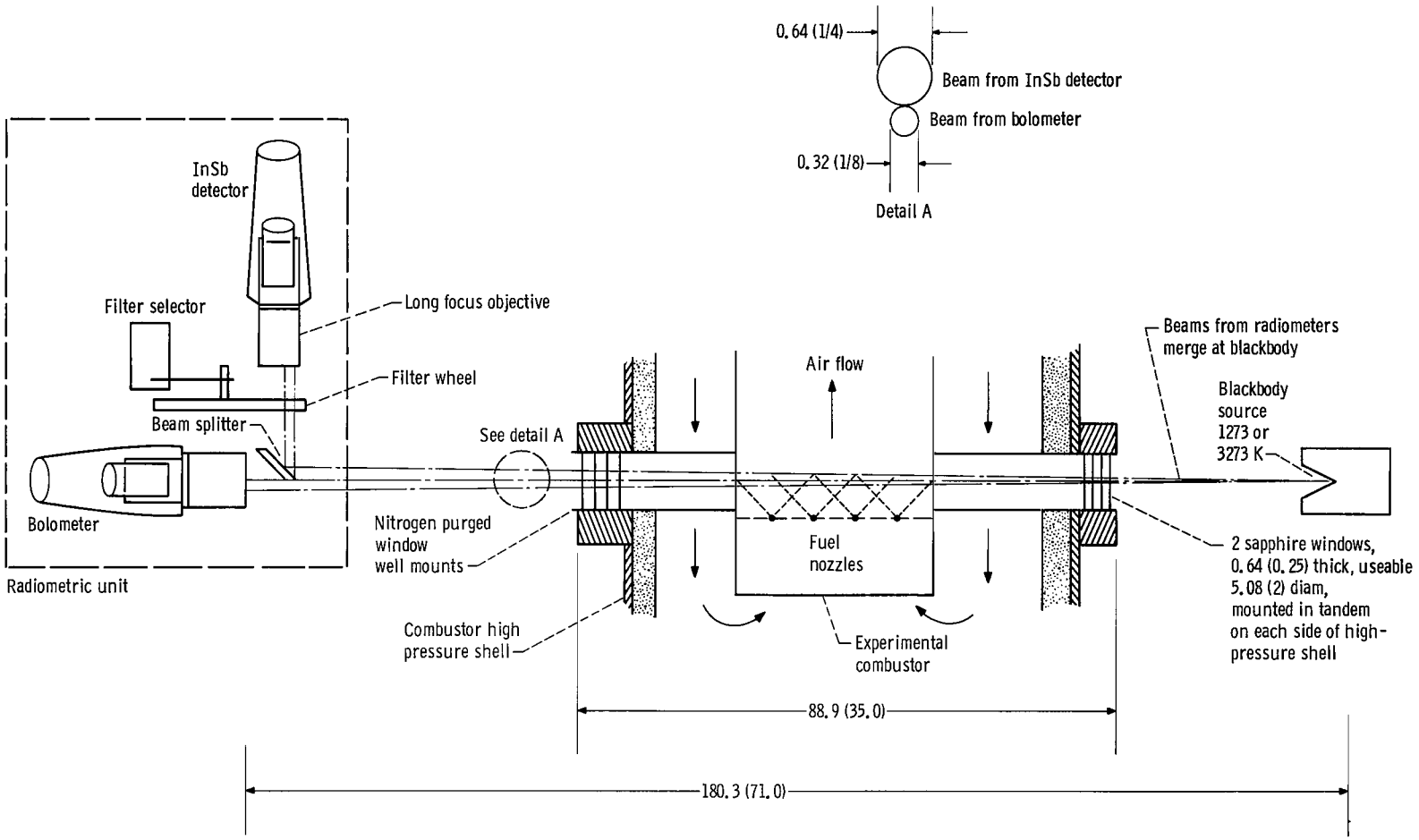

Figure 6. - Infrared measuring system for determination of smoke concentration and total radiance. Dimensions are in cm (in.)).

Optical system. - The optical system external to the radiometer is shown in figure 6. All components were mounted on two 10.16-centimeter (4-in.) I-beam sections bolted with reference to the combustor fuel nozzle location. The desired spectral bandwidth interference filter for the indium antimonide detector could be selected by means of a remotely controlled filter wheel assembly. A blackbody calibration source was mounted opposite to the radiometric unit. Dual sapphire windows (for IR transmission) 5.72 centimeters (2.25 in.) in diameter and 0.64 centimeter (0.25 in.) thick were used on each side of the combustor housing to contain the combustion process and to view the flame at a position 5.08 centimeters (2 in.) downstream of the fuel nozzles. The four windows presented eight surfaces through which the blackbody reference source was viewed and four surfaces through which the smoke was viewed. It was experimentally established that within the limits of parallelism encountered, due to mounting and random rotational positioning of the windows, no appreciable attenuation of the signal was observed. The individual windows were specified to be parallel to within 0.0025 centimeter (0.001 in.) with a flatness of one-tenth wave.

The radiometric unit position at the first window location was optimized during preliminary checkout by observing the maximum total radiance. Peak intensity occurred about 5.08 centimeters (2 in.) downstream of the fuel nozzles and this position was fixed for all subsequent tests.

The optical system has two nitrogen purge systems: (1) a low-pressure purge, which was used to eliminate atmospheric absorption during operation, and (2) a high-pressure nitrogen purge within the window well mounts on the high-pressure combustion side. This flow minimized the effect of combustion product recirculation into the window well mounts and kept the temperature of the window seals at a safe level. The radiometer case had provision for water cooling in addition to the nitrogen purge so that radiometric components would be maintained at a uniform temperature level.

Spectral filters. - The filters selected for the spectral radiance measurements were centered at bypass bandwidths of 2.70 and 4.05 micrometers.

The transmission curves and the indicated half-height bandwidth of the two filters are presented in figure 7. The bandwidth of the interference filter is usually specified at half of the peak transmission height of the filter in order to avoid the relatively undefinable region associated with the lower wings of the transmission curve. As shown in figure 7, these filters have a relatively sharp cutoff of the wings at the base of the transmission curve. The half-height bandwidths for the 2.70- and 4.05-micrometer filters are 2.608 to 2.789 and 4.015 to 4.085 micrometers, respectively. No measureable transmission leakage occurred through the filters as indicated by the spectrophotometer plot (fig. 7) out to 6 micrometers which is the cutoff region of the sapphire windows used in the optical system.

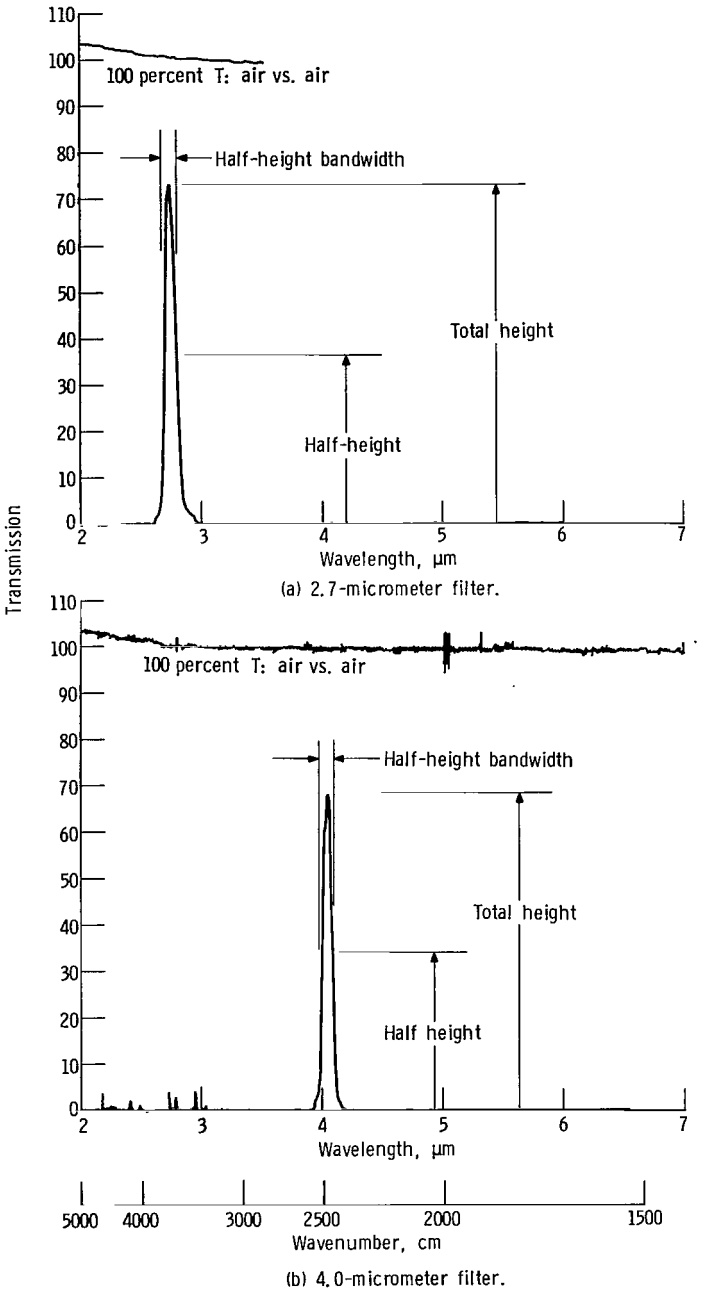

(a) 2.7-micrometer filter.

(b) 4.0-micrometer filter.

Figure 7. - Transmission curves for 2.7- and 4-micrometer interference filters.

Calibration. - Each radiometer was calibrated by viewing a blackbody reference source at a target distance of 1.80 meters (71 in.) from the radiometric unit. The radiometer and blackbody could be positioned independently in the x, y, and z directions. The system was visually alined and focused at the optical viewing head. Final alinement was accomplished by monitoring the output from each radiometric head and peaking the signals.

The blackbody reference source was monitored by means of a calibrated extinction pyrometer and thermocouple for temperature levels up to 1273 K. Above this temperature the extinction pyrometer was supplemented by a modified two-color pyrometer. Two blackbody sources were used to cover the required temperature range: a low-temperature blackbody (1273 K) with the 2.54-centimeter (1-in.) diameter cavity resistance heated and the temperature level controlled electronically, and, for temperature levels to 3273 K, an induction heated furnace as described in reference 33. This source has a 0.953-centimeter (0.375-in.) diameter blackbody cavity. The source was modified from the original design by substituting an yttrium-stabilized, course-grained, fused zirconium oxide insulator to improve recycling fatigue. In addition, a dry-nitrogen-purged enclosure was added to reduce the oxidation of the carbon rod.

The various components in the optical system, such as the detectors, filters, sapphire windows, etc., do not have an ideal flat spectral response over all wavelengths. When the infrared detector or collecting optics do not have an ideally flat spectral response, transmission, or reflection, it is helpful to define the term "effective blackbody radiance." Effective blackbody radiance is a normalized radiance that takes into account the nonflat spectral characteristics of the complete system (fig. 6). Effective blackbody radiance is linearly related to the radiometer electric output and is defined as

$$L_{B,\,eff} = \int_0^\infty \frac{N_{(\lambda)}}{N_{peak}} L_{B(\lambda)} d\lambda \tag{14}$$

where $N_{(\lambda)}$ is equal to the detector response, N_{peak} the peak detector response, and $L_{B,\,eff}$ the blackbody radiance evaluated from the Planck function. Values of $L_{B,\,eff}$ are computed for various blackbody temperatures using the spectral response of the radiometer detector and optics. A curve of $L_{B,\,eff}$ as a function of blackbody temperature is supplied by the manufacturer with the instrument for each combination of optics. These curves were verified by determining the spectral response of each of the system components.

Since the effective blackbody radiance is linearly related to the signal, the constant of proportionality can be determined by calibration with the blackbody source. Initially, a constant was obtained for each radiometer and filter combination in a series of temper-

ature steps up to 2873 K. After the appropriate constants were established, a check point at 1123 K was taken before and after each experimental test. In this manner it was possible to ascertain if smoke from the combustor had recirculated and deposited on the relatively cool window surface and, if so, to what extent the calibration changed during the test run.

The blackbody temperature from the radiometer output is determined by the following procedure: (1) the output voltage is recorded from the digital voltmeter, (2) the voltage is multiplied by the instrument constant to obtain effective blackbody radiance, and (3) the blackbody temperature is determined from the calibration curve of effective blackbody radiance as a function of temperature furnished by the manufacturer. The actual radiance can be calculated from the blackbody temperature and wavelength interval as described in the ANALYTICAL TECHNIQUE section. For each test of reported data, three radiometric readings were required as shown in table I.

TABLE I. - RADIOMETRIC MEASUREMENTS

Nominal wavelength, μm	Actual half-height bandwidth, μm	Type of detector
Total spectral	0.25 to 6.0	Bolometer
2.7	2.608 to 2.798	Indium antimonide
4.05	4.015 to 4.085	Indium antimonide

Smoke Number Measurement

The smoke sampling procedure as recommended in reference 28 was followed as closely as possible. A movable, water-cooled platinum rake is used to survey the exhaust gas to determine combustor operating parameters such as combustion efficiency and temperature profile. This probe was used to obtain the exhaust gas smoke sample. A photograph of the probe sampling head is shown in figure 8. The probe is of the aspirating type with five 0.64-centimeter (0.25-in.) diameter ports located in the exit plane evenly spaced over a total vertical height of 5.08 centimeters (2 in.). Exhaust gas is aspirated to atmospheric pressure past thermocouples located within the tubes. The five tubes are combined into one 0.95-centimeter (0.38-in.) diameter stainless steel manifold tube maintained at a temperature level above the dew point of the exhaust gas. It would be expected that, because of the small size of the smoke particles, they would follow the stream and that a representative smoke sample would be obtained. The

Figure 8. - Exhaust rake used to obtain smoke samples. (Dimensions in cm (in.).

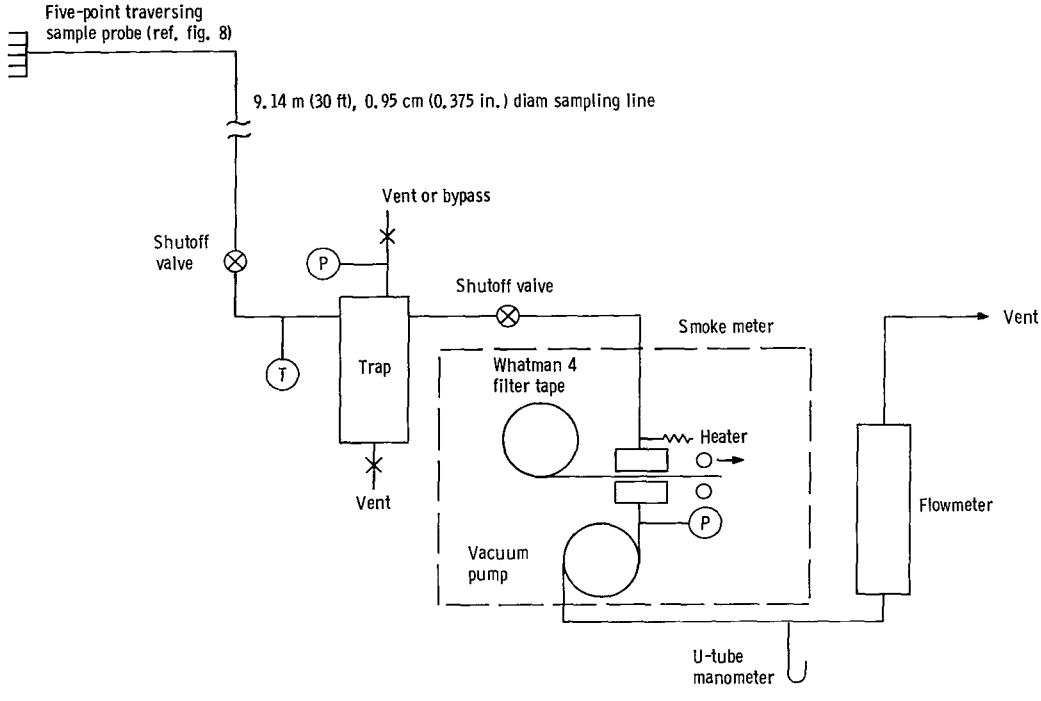

Figure 9. - Exhaust smoke sampling system.

smoke sample was obtained 33.02 centimeters (13 in.) from the fuel nozzles at a station corresponding to the turbine position in an advanced combustor design.

A continuously stained filter tape record was obtained as the probe was surveyed at the exhaust station. A schematic of the smoke metering equipment is shown in figure 9. The volumetric flow rate of the smoke sample was similar to that used in reference 18 and 29. In operation, a smoke sampling rate of 0.28×10^{-3} cubic meter per second ($0.6\ ft^3/min$) was used to stain the filter paper, and the remainder of the sample bypassed to the exhaust system. The filter paper tape moved at the rate of 0.17 centimeter per second (4 in./min) with a smoke trace 1.27 centimeter (0.5 in.) wide. The tape was placed on a black background tile to measure comparative reflectance readings required to determine smoke number.

RESULTS AND DISCUSSION

The combustor was operated at test conditions typical of those encountered in a turbojet engine with a 20:1 compression ratio at takeoff and cruise. The combustor inlet air was heated to 589 K (1060° R) by means of an indirect fired preheater. To attain a temperature level of 756 K (1360° R), it was necessary to vitiate the air by burning methane fuel upstream of the combustor. Four test points were selected as shown in table II. In general, each test condition was operated over a range of fuel-air ratios with an ASTM-A1 type of fuel. An analysis of the fuel is shown in appendix C.

TABLE II. - COMBUSTOR TEST CONDITIONS

Inlet pressure, atm	Inlet temperature		Combustor reference velocity	
	K	$^{\circ}$R	m/sec	ft/sec
10	589	1060	21.3	70
	756	1360	27.3	90
20	589	1060	21.3	70
	756	1360	27.4	90

Smoke Concentration

Primary and exhaust smoke concentrations. - The spectral radiance from the smoke cloud was converted to the concentration of smoke particles in the primary combustion zone, and the smoke number at the exhaust station was converted to the smoke concentration at the exhaust plane. The smoke concentrations in the primary zone and the smoke concentration and corresponding smoke number at the exhaust station are shown in figure 10 for three representative combustors.

The smoke concentrations are presented only for a single value of inlet air temperature of 589 K (1060° R). The indicated smoke concentration in the primary zone ranged from 5.3×10^{-7} to 5.8×10^{-6} gram per cubic centimeter, and at the combustor exhaust station the smoke concentration ranged from 1.8×10^{-10} to 1.5×10^{-8} gram per cubic centimeter for the three combustor configurations.

The smoke concentrations in the primary zone for the three combustors were approximately 100 to 1000 times greater than observed at the exhaust. This holds for the smoky combustor model A as well as the relatively clean combustors models B and C. The difference in the primary smoke concentrations between a smoky and clean combustor was less than a factor of ten. These results indicated that an appreciable amount of carbon is formed in the primary combustion zone even for a clean configuration and that 99 percent or more of the carbon formed is burned before it is exhausted.

A high primary smoke concentration has also been observed in a low-pressure combustor which produced no visible smoke (ref. 3). The threshold of visible smoke is a rather arbitrary designation in that viewing conditions and depth of plume effect visibility. In general, the smoke number level associated with the visible threshold is in the range from 20 to 30 (6.4×10^{-9} to 9.9×10^{-9} g/cm^3) for a plume approximately 60.96 centimeters (2 ft) in diameter as discussed in reference 34. In the combustor of reference 3, the primary zone could be readily sampled because of the low total-mass concentration of smoke formed at the operating pressure of 1.36 atmospheres. An average primary smoke concentration of 1.8×10^{-6} gram per cubic centimeter was indicated even though no measurable smoke was detected at the exhaust. The method of determining the smoke concentration at the exhaust was sensitive to 1.0×10^{-8} gram per cubic centimeter. This would indicate that a factor of at least 180 existed between the primary and exhaust smoke concentration for low-pressure operation. The program was not continued at higher pressure levels because the sample probes became plugged.

The present study at high combustor pressures indicates from inferred smoke measurements that in general a similar magnitude of smoke concentration exists between the primary and exhaust stations, as compared with the referenced combustor operating near atmospheric pressure. It should be noted that the smoke density is reduced to standard volumetric gas measurement conditions. It is also to be noted that dilution

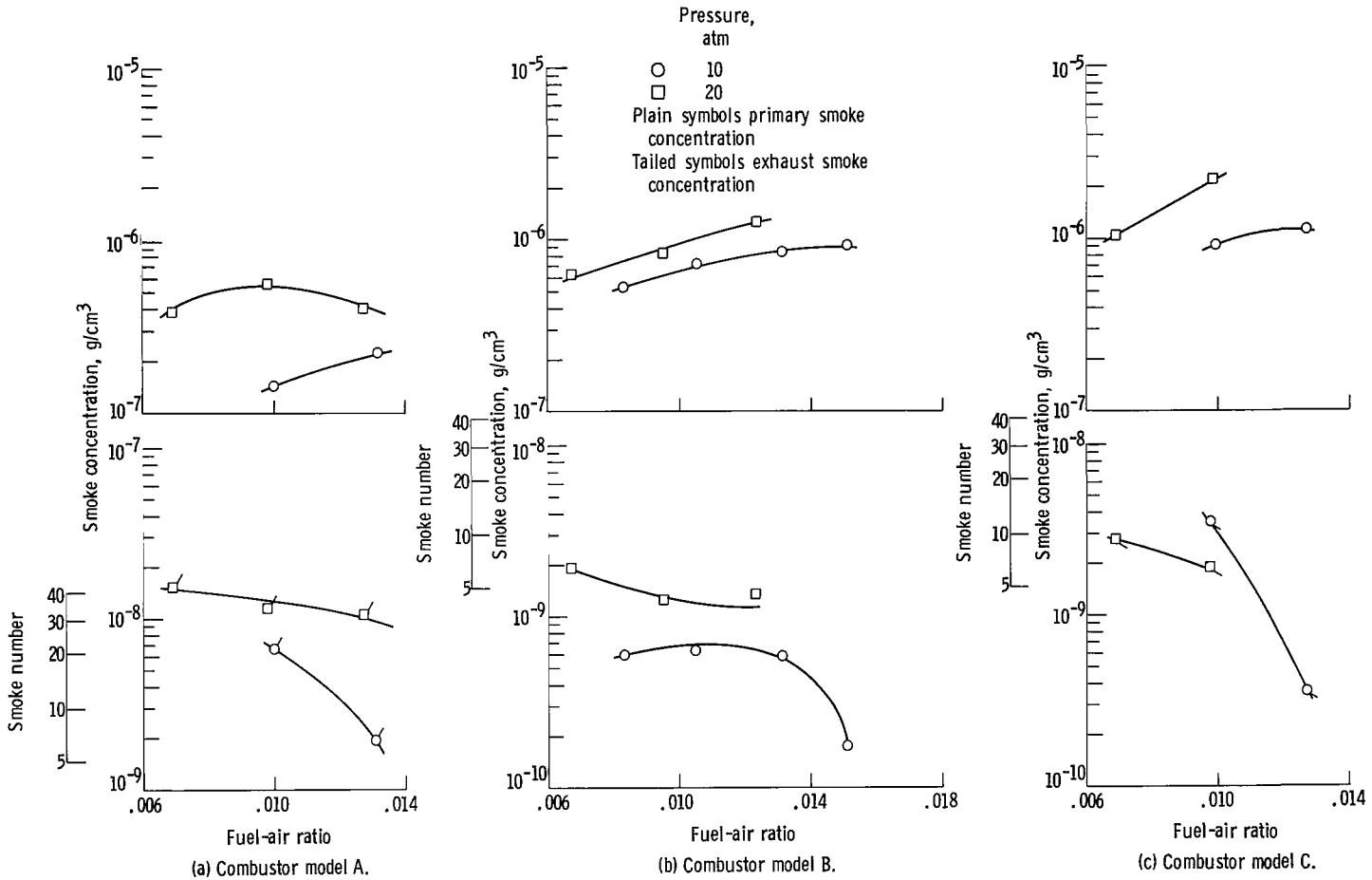

Figure 10. - Calculated smoke concentrations for three experimental combustor configurations. Inlet temperature, 589 K (1060° R); reference velocity, 21.3 meters per second (70 ft/sec).

effects reflected in the exhaust gas due to secondary air addition have not been separated.

As shown in figure 10 there was a tendency for the primary smoke concentration to increase with increasing fuel flow as would be expected. As a larger quantity of fuel is burned there would be a greater opportunity for smoke formation if it is assumed that the kinetics of smoke formation remain similar.

The level of smoke concentration at the exhaust did not increase with increasing fuel flow as would be expected. Rather, there was an actual decrease in smoke concentration. It is believed that the unique combustor design inherently exhibited this characteristic due to the influence of the flame temperature. This effect is brought about by the manner in which primary air required for complete combustion of the fuel at maximum flow is admitted concentric to the fuel nozzles. At the low fuel-flow condition, the pressure drop across the fuel nozzle is low, so that a poor fuel spray is produced. This coarse spray is mixed with a large excess of air and, at low fuel flows, apparently the turbulence is not sufficient to prevent locally over-rich regions around the fuel droplets from being formed. The observed low flame temperature results. At higher flows the fuel nozzle is operating in the design regime with respect to atomization and the local fuel-air ratio is nearer stoichiometric. The flame temperature increases at these higher fuel flows, and less smoke is found in the exhaust sample. The higher temperature associated with increased fuel-air ratio is responsible for the increased consumption of carbon formed in the primary zone so that less is observed at the exhaust.

Combustor exhaust smoke number. - The exhaust smoke numbers obtained for the three experimental combustor configurations are presented in figure 11. The smoke number (1) increased as the combustor pressure increased except for the higher inlet temperature and reference velocity of combustor C, (2) decreased as the inlet temperature and reference velocity increased, and (3) decreased as the fuel-air ratio increased. The first two trends are similar to those observed in previous studies as shown in references 35 and 36. The decrease in smoke concentration with an increase in fuel-air ratio was considered characteristic of the experimental combustor configuration. For the most severe smoking condition tested (20 atmospheres pressure and 589 K (1060° R)), the smoke numbers ranged from 40 to 32, 6 to 4, and 9 to 5 for combustor models A, B, and C, respectively.

order of 20 to 30. Combustor model A would generate a visible exhaust plume (range of the order of 40 to 32). A smoke number of 40 is associated with a smoke concentration of 1.41×10^{-8} gram per cubic centimeter as shown in figure 10. This concentration corresponds to 0.16 percent of the total carbon present in the fuel converted to the smoke cloud. It is apparent that this quantity of unburned carbon would not be reflected in combustion inefficiency and that only a small fraction of carbon in the form of smoke will give rise to an unsightly smoke plume.

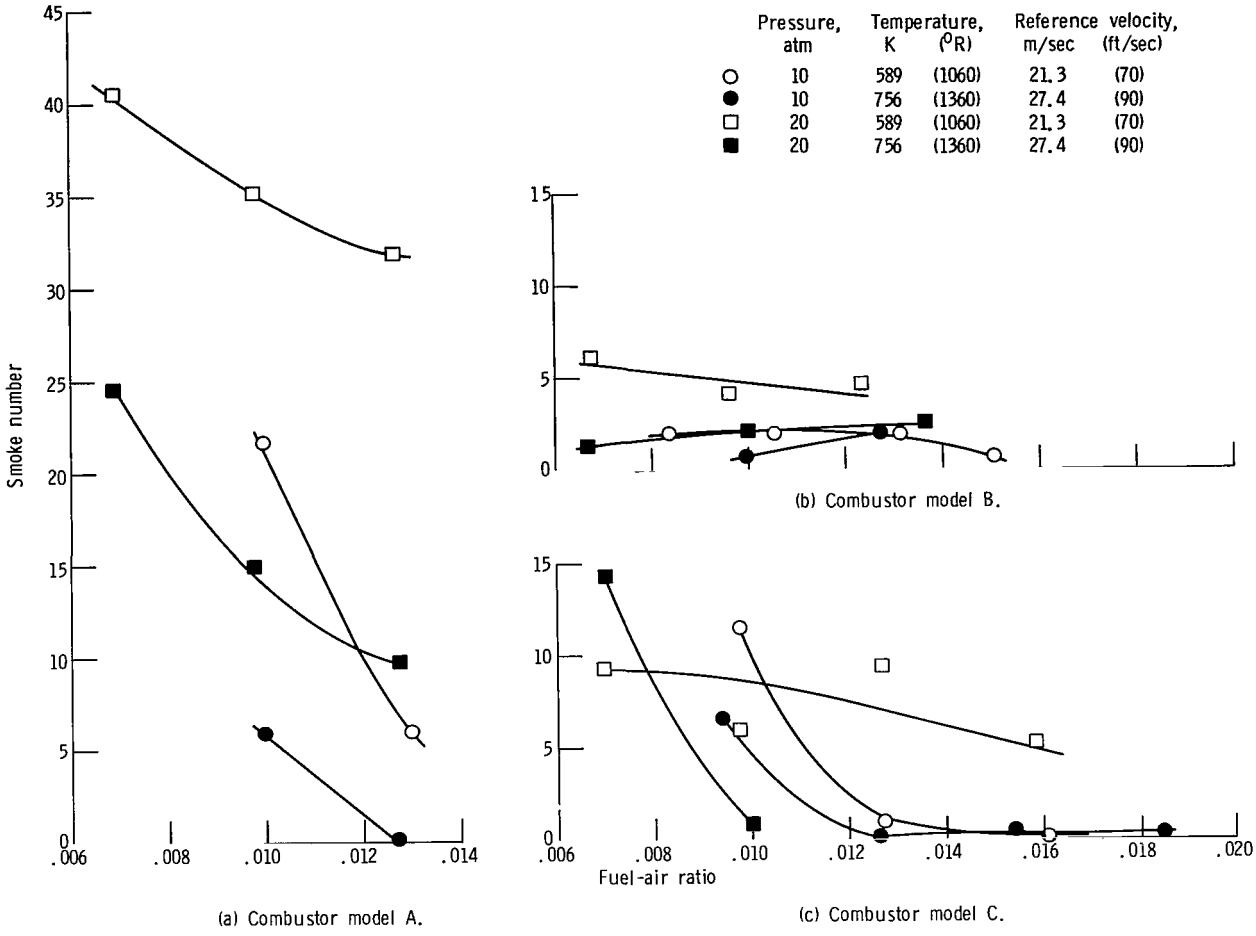

Figure 11. - Exhaust smoke number determination for three experimental combustor configurations.

Thus major improvements in smoke emission levels can be effected through application of existing design principles even for a highly efficient combustor.

Oxidation of Smoke

It was shown that 99 percent or more of the carbon converted to smoke in the primary combustion zone is burned within the combustor. The concentration of carbon present for a smoke number of the order of 20 to 30, which is associated with the visible threshold of a smoke plume, is 6.4×10^{-9} to 9.9×10^{-9} gram per cubic centimeter. A small increase in the concentration can influence the visibility of the smoke to a marked degree. It is of interest to the combustor designer to be able to estimate the amount of smoke that can be consumed by the oxidation of smoke within the combustor. An attempt

was made to correlate the oxidation of smoke within the combustor in a manner similar to that formulated in references 23 and 24 for the oxidation of a very small carbon particle seeded in a laboratory flame. In reference 37 the relative oxidation rates have been compared with the data of references 23 and 24 with respect to gas turbine combustor conditions. It was shown that carbon oxidation within the combustor plays an important role in determining the smoke emission level of an engine.

Specific reaction rate. - The specific reaction rate was calculated from the primary

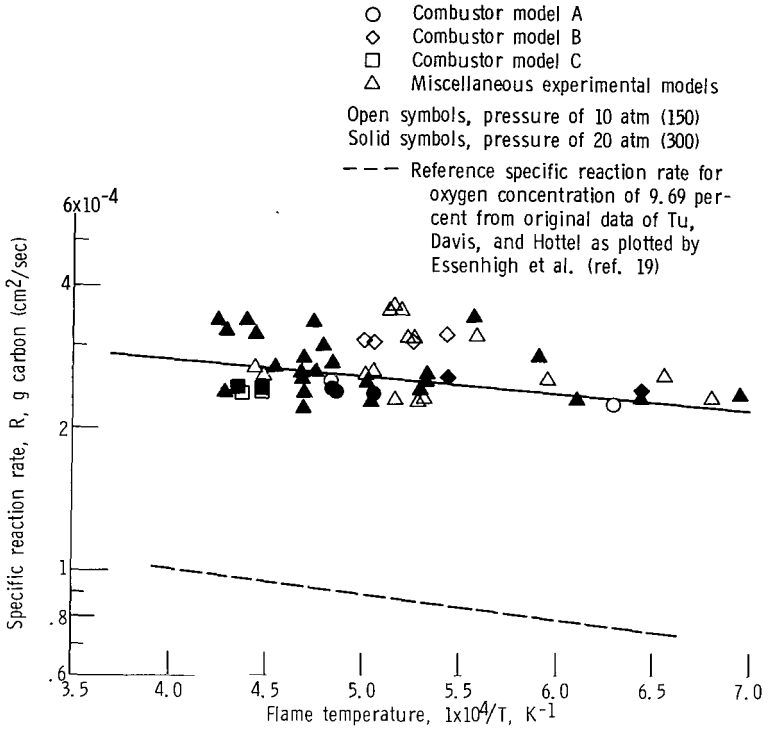

Figure 12. - Arrhenius plot of specific reaction rate for 10 experimental combustors.

and exhaust smoke concentration. An Arrhenius plot of the specific reaction rate as a function of the observed flame temperature is shown in figure 12. The data from the three reference combustors and seven additional combustor configurations are included. The specific reaction rate is of the order of 2.5×10^{-4} grams carbon per square centimeter per second for 10 experimental combustor configurations operated at 10 and 20 atmospheres for an average flame temperature of 2000 K (3600° R). The observed flame temperature in general increased as the operating fuel-air ratio increased; however, the flame temperature was strongly dependent on the combustor configuration.

Specific reaction rate considerations. - The oxidation of the carbon coal particle

has been reviewed by Essenhigh, et al., in reference 19. A surface reaction is assumed which is dependent on (1) diffusion, (2) adsorption of the reacting gas, and (3) desorption of the products. It has been shown that for particles less than 100 micrometers the reaction is not controlled by a diffusional boundary layer, therefore, for the oxidation of smoke within the combustor the diffusion processes can be neglected. The rate determining steps are thus associated with the chemical reaction of the solid surface. Langmuir has treated adsorption in a unimolecular layer from the standpoint of the equilibrium between gas molecules striking the surface and those that evaporate after a given time. Since the number of molecules that strike a surface is proportional to the pressure p and assuming that k_1 and k_2 are constants for a given system, the reaction rate can be expressed (as used in ref. 19) as

$$\frac{1}{R_L} = \frac{1}{k_1 p_{0,2}} + \frac{1}{k_2} \tag{15}$$

where k_1 is the velocity constant for adsorption and k_2 is the velocity constant for desorption.

The velocity constants can be expressed as follows

$$k_1 = A_1 \exp\left(-\frac{E_1}{RT}\right) \tag{16}$$

$$k_2 = A_2 \exp\left(\frac{E_2}{RT}\right) \tag{17}$$

If the reaction controlling step is assumed to be adsorption E_1 is of the order of 8368 joules per mole (2000 cal/mole), and if the reaction controlling step is assumed to be desorption E_2 should have a value of 167 360 joules per mole (40 000 cal/mole) as discussed in reference 19.

From the Arrhenius plot (fig. 12) the energy associated with the oxidation of the combustor smoke is of the order of 7322 joules per mole (1750 cal/mole). It should be noted that because of data scatter it is difficult to establish an absolute value for the energy level; however, a very low energy level is indicated. Included in figure 12 is a curve for the oxidation of coal particles taken from reference 19 for an oxygen concentration of 9.69 percent. A similar slope corresponding to 8368 joules per mole (2000 cal/mole) is indicated.

The oxidation of smoke within the combustor did not show any particular trend with respect to the partial pressure of oxygen. A change in reaction rate level would be

expected because of the change in the partial pressure of oxygen at different combustor operating pressures. Results on the seeding and burnup of carbon in a laboratory flame have indicated that at the present time the reaction mechanism has not been established. In reference 23 a dependency on molecular oxygen was observed, but in reference 24 no such dependency was noted.

It was not possible in the present combustor application study to control the variables of flame temperature and the concentration of reacting species to the degree required to evaluate the reaction mechanism.

The specific reaction rate is compared with the rates obtained from the literature as shown in table III. Comparison was made at a temperature of 2000 K (3600^{o} R).

TABLE III. - COMPARISON OF SPECIFIC REACTION RATE

Specific reaction rate, gm/cm^2 sec	Energy associated with reaction		Dependency	Comments	Reference
	J/mole	cal/mole			
2.5×10^{-4}	7 322	1 750	Insufficient data; relatively independent of oxygen	Combustor smoke oxidation at 10 to 20 atm	This report
3.1×10^{-5}	8 368	2 000	Oxygen dependent	Evaluated from original data of ref. 20 2.98 percent oxygen	19
5.0×10^{-4}	164 431	39 300	Oxygen dependent	Seeded laminar flame	23
16.0×10^{-4}	92 048	22 000	Independent of oxygen, OH dependent	Seeded laminar flame	24
7.0×10^{-4}	4 184	[a]1 000	Carbon + air	Carbon + CO_2 tended to reduce reaction rate	39

[a]Estimated.

Because many of these studies did not encompass this range, a linear extrapolation was made to estimate the reaction rate.

The data from reference 24 indicated that the energy associated with the reaction was of the order of 92 048 joules per mole (22 000 cal/mole). This value is considerably higher than that indicated from the combustion data. Variation in the energy associated with the oxidation of coal particles has been experienced by numerous investigators, (e.g., refs. 38 and 39). Golvina and Khaustovich in reference 39 have shown that the reaction rate rose rapidly up to about 1000 K (1800^{o} R), in agreement with Tu (ref. 20), then leveled off over the temperature range to 1400 K (2520^{o} R). It rose rapidly again over the range from 1400 to 1750 K (2520^{o} to 3150^{o} R) and then leveled off again up to 3000 K (5400^{o} R). The flame temperature levels reported in reference 24

covered a range from 1530 to 1890 K (2750° to 3400° R), but the range of combustor flame temperatures were primarily in the range from 1800 to 2700 K (3240° to 4860° R). Therefore, it is possible that, at the higher temperature level, a drop in energy could occur as reported in reference 39.

The phenomena associated with the oxidation of a carbon particle indicates that the combustion is dependent on temperature. Recent work has shown that the heat released during the oxidation of the particle may change the temperature of the particle itself independent of the gas stream (ref. 38). Thus, a thermocouple immersed in the stream or a measurement of temperature based on the stream would not necessarily be reliable in estimating the particle temperature. Using this approach, a particle model experiencing a time varying temperature gradient was postulated that could possibly explain the anomolies experienced by previous investigators. Further work will be required to examine the detailed processes that are envolved during the oxidation of the particle and application to combustion problems.

The reaction rate determined from the experimental combustor study appears to be somewhat lower than most of the rates previously observed. Part of the difference may be due to the manner in which the residence time is calculated. The combustor reference velocity was used because it has been shown that performance characteristics among many different types of combustors can be related to this parameter. The actual flame velocity was not determined because of uncertainty in defining the flame recirculation pattern. Another variable that will influence the magnitude of the reaction rate is the initial particle diameter. No attempt was made in this investigation to independently determine initial particle size. Data in the literature indicate that a range from 5×10^{-7} to 6×10^{-6} centimeter may be obtained. As previously mentioned, the initial particle diameter selected (1×10^{-6} cm) was based on the value reported in reference 24.

Total Radiant Heat Flux and Flame Emissivity

The total radiance from the flame was obtained to determine the heat flux load on the combustor liner due to flame radiation.

Total radiance. - The total spectral radiance obtained from the flame in the primary combustion zone is shown in figure 13 for three combustor configurations. In general, the total flame radiance increased as the combustor pressure and fuel-air ratio increased. Comparison at a fuel-air ratio of 0.014 indicated that as the pressure was increased from 10 to 20 atmospheres, the radiance increased from 25.5 to 38, 10.2 to 14.3, and 16.6 to 28.7 watts per square centimeter per steradian (80 to 120, 32 to 45, and 52 to 90 $(Btu/(hr)(ft^2)(sr))\times10^3$) for combustor models A, B, and C, respectively. The smoky combustor A had the highest level of radiance, and the cleanest combustor B

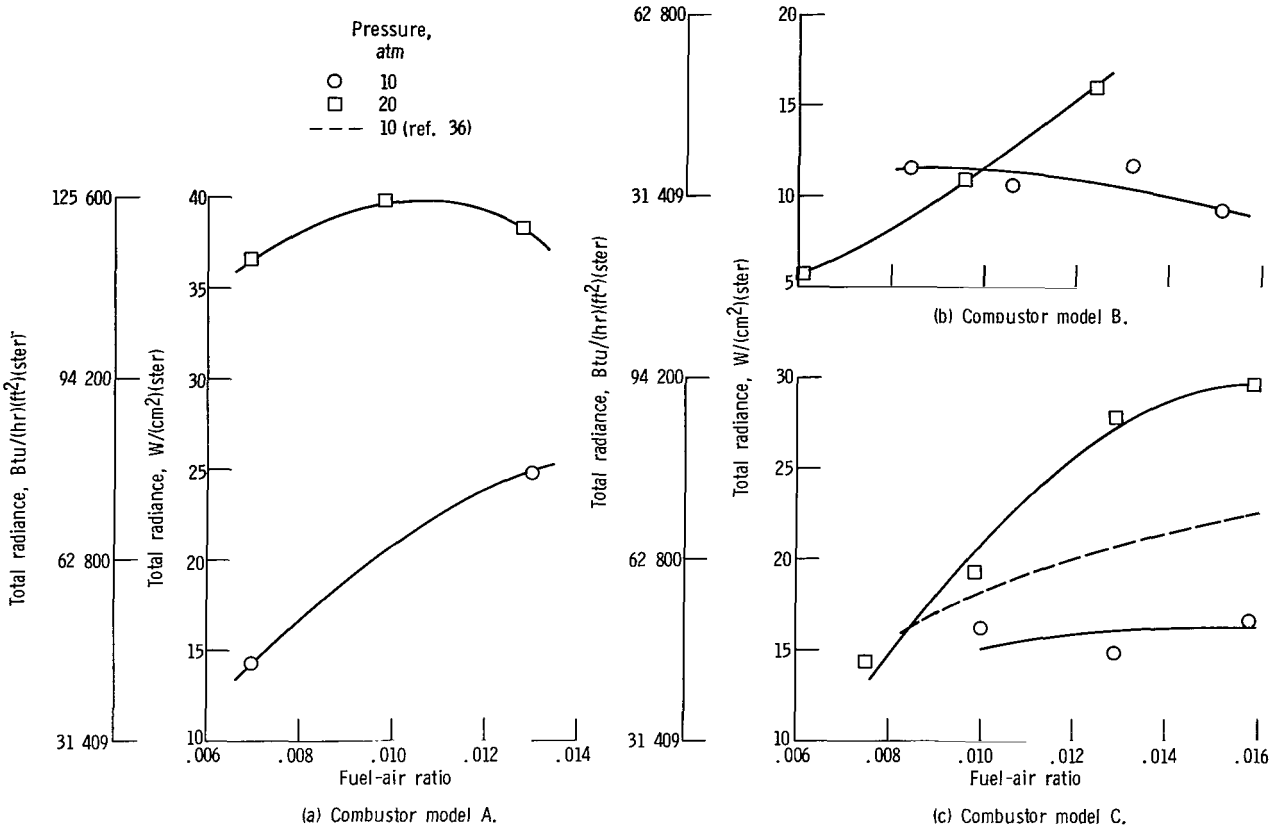

Figure 13. - Total radiance monitored at primary zone for three experimental combustor configurations. Inlet temperature, 589 K (1060° R); reference velocity, 21.3 meters per second (70 ft/sec).

had the lowest level. It is to be noted that radiance is expressed as radiant power per unit solid angle per unit projected area. The total hemispherical blackbody emissive power is π times the directional emissive power normal to the surface.

The small scale 5.08-centimeter (2 in.) combustor from reference 36 is included for comparison with figure 13(c). The reference combustor was operated (1) with ASTM A-1 fuel, (2) at a pressure level of 10 atmospheres, (3) at a high velocity (data indicated that radiation from this combustor was insensitive to velocity), and (4) at an inlet temperature of 544 K (1160° R). These data are compared with combustor model C operated at 10 atmospheres at an inlet temperature of 589 K (1060° R). In general the trend of increasing radiance with fuel-air ratio obtained with the reference data was similar to that obtained in the present study.

For combustor model C, the 10-atmosphere pressure condition, and a fuel-air ratio of 0.010 the corresponding blackbody radiance of the flame at a temperature of 2250 K (4050° R) is of the order of 46.3 watts per square centimeter per steradian (154×10^3 Btu/(ft^2)(hr)(sr)). Combustor model C operated at a total radiance level of the order of

16.6 watts per square centimeter (52×10^3 Btu/(ft^2)(hr)(sr)) which is approximately one-third the value of an equivalent blackbody radiator.

Smoke number and total radiation relationship. - The total radiance was observed to be higher with a smoky combustor than with a clean configuration. Radiation data from the three combustor configurations are compared with respect to the exhaust smoke number in figure 14 at a combustor operating pressure of 10 and 20 atmospheres and an inlet temperature of 589 K (1060° R). The total radiance and smoke number data were extrapolated as required to present values at a constant fuel-air ratio of 0.014. A fuel-air ratio of 0.014 corresponds to a temperature rise level of approximately 556 K (1000° R) and represents values of interest for takeoff and cruise conditions. Lower operating fuel-air ratios would cause a departure from the relationship of figure 14 since the observed differences in total radiance are due to the combination of primary-zone smoke concentration and flame temperature (i.e., lower fuel-air ratios result in lower overall flame temperature). It has been previously shown in figure 13 that increasing fuel-air ratio tends to increase the total radiance; therefore, the region of greatest interest lies in the higher fuel-air ratio range. The fuel-air ratio of 0.014 was selected for comparison because most of the combustor configurations could be

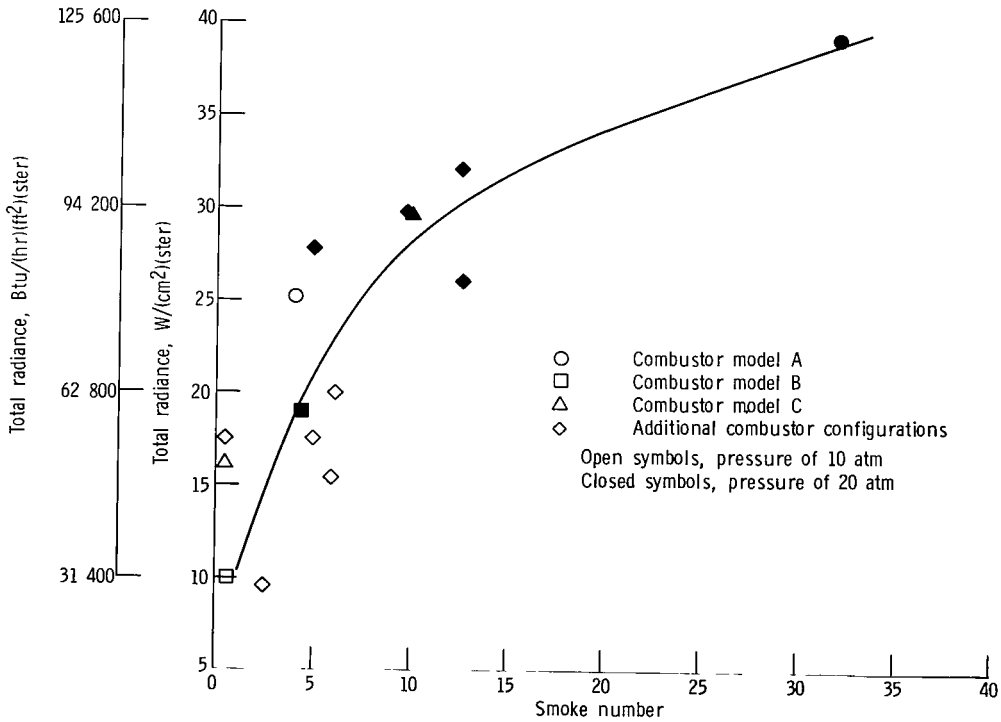

Figure 14. - Total radiance and exhaust smoke number relationship. Fuel-air ratio, 0.014; inlet temperature, 589 K (1060° R); reference velocity, 21.3 meters per second (70 ft/sec).

readily operated to this level without causing local over-temperature indications on the exhaust instrumentation probe.

As the exhaust smoke number increased, the total radiance in the primary zone increased. The increase in radiance over the range of measured smoke numbers appears to be relatively insensitive to combustor operating pressure as shown in figure 14. It should be noted for the 10 atmosphere pressure that the experimental combustors operated with a smoke number of less than 10. Consequently, higher smoke numbers are only associated with the 20 atmosphere condition. Comparison of the three combustor configurations shown in figure 14 indicate approximately a threefold reduction in total radiance as the exhaust smoke number was reduced from 32 to 2. Data from several additional combustor configurations are also included, and a similar relationship is observed.

The primary zone smoke concentration and flame temperature, which determine total radiance, are dependent on many factors including combustor operating parameters, fuel-air ratio, and the degree of mixing. A relatively high combustion efficiency was obtained for all of these combustors, however, the observed flame temperature was not similar because of combustor design variables. The measured flame temperature for the conditions corresponding to the data in figure 14 at 20 atmospheres are 2230, 2040, and 2200 K (4014°, 3672°, and 3960° R), for models A, B, and C, respectively. Thus, even though identical operating conditions were compared and high combustion efficiency was obtained, additional measurements are required to calculate total radiance since combustion flame temperature can not be assumed to be constant for different combustors.

The design engineer is interested primarily in the effective total radiance in order to estimate liner cooling requirements. The exhaust smoke number criterion appears to be a good simple guide for a first approximation to estimate the total radiation level of the flame for different combustor configurations (see fig. 14). A general combustor design goal is to reduce the exhaust smoke to the threshold of visibility. Assuming this condition to be represented by a smoke number of 25, the corresponding total radiance is 36.2 watts per square centimeter per steradian (113 670 Btu/(hr)(ft^2)(sr)). It should be noted that an appreciable reduction in total radiance to the liner is possible if the exhaust smoke level is reduced far below the visible threshold. In actual design practice, however, this may not be wise because of the consideration of altitude relight capability.

Total flame emissivity. - The total radiance from the flame is determined by the flame emissivity and temperature. In this investigation the flame temperature and total radiance were experimentally determined. The flame emissivity calculated from the observed temperature and radiance is presented in figure 15 for the three combustor configurations. The total flame emissivity increased as the combustor pressure in-

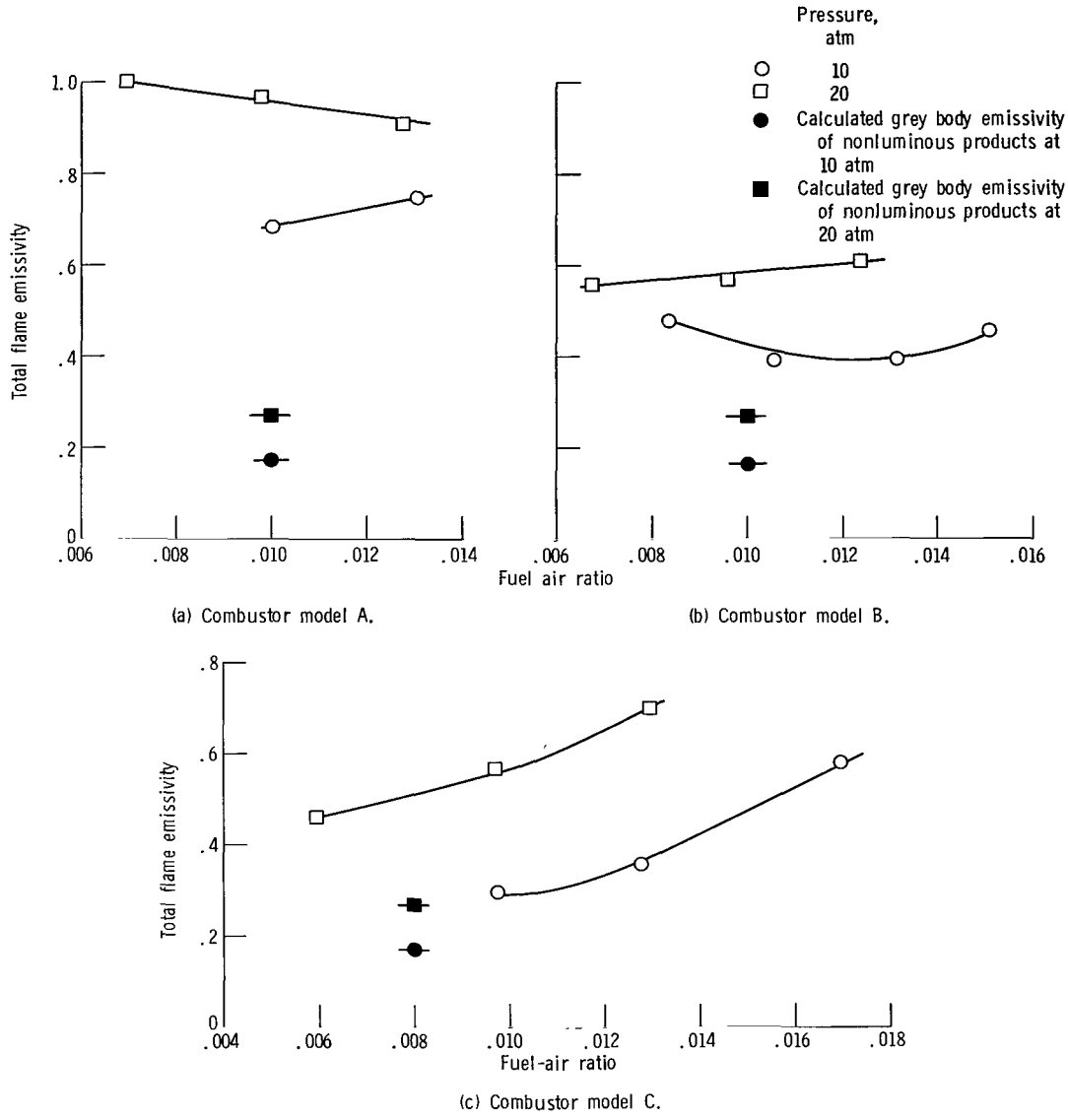

Figure 15. - Total flame emissivity calculated at the primary zone for three experimental combustor configurations. Inlet temperature, 589 K (1060° R); reference velocity, 21.3 meters per second (70 ft/sec).

creased from 10 to 20 atmospheres for a constant inlet temperature of 589 K (1060° R). At a combustor pressure of 20 atmospheres and a fuel-air ratio of 0.014, the flame emissivity was 0.9, 0.6, and 0.73 for combustor models A, B, and C, respectively. The measured flame temperatures for these emissivities correspond to 2230, 2040, and 2200 K (4014°, 3672°, and 3960° R), respectively.

The total emissivity of the nonluminous combustion products at an equivalence ratio of 1 is shown for comparison in figure 15. The emissivity was estimated from the

greybody approximation technique as proposed by Hottel and discussed in reference 40. This method is used to represent the band radiation as determined from the ideal products in terms of an equivalent greybody radiator. The equivalent greybody emissivity associated with water vapor and carbon dioxide at 20 atmospheres is 0.27. Comparison of nonluminous and total emissivity indicate that the increase in emissivity is due to the inclusion of radiating smoke particles. It is these smoke particles that are responsible for most of the radiant heat from the flame at high pressure levels.

If no smoke is formed, the radiation level will approach that due to radiation from the nonluminous products alone. In practice, however, it is more likely that the radiation level would be considerably higher due to smoke and could approach that of a blackbody radiating at flame temperature.

Combustor design, however, can reduce total flame emissivity substantially as shown in figure 15.

The range in total flame emissivity from figure 15 is compared in figure 16 with the flame emissivity reported for kerosene fuel from reference 41. The data from reference 41 are limited to 10 atmospheres pressure, and the data from figure 15 were taken at a fuel-air ratio of 0.014. As the combustor pressure is increased to 20 atmospheres it is shown that emissivity tends to level out. The combustors in this investigation produced less smoke at the exhaust than is normally encountered in current practice. Even so, it is apparent that a wide range in flame emissivity was measured. The lowest emissivity was of the order of 0.6 at 20 atmospheres pressure. Advanced combustor designs using pressure atomized fuel should be capable of achieving this level of emissivity. Detailed liner cooling heat-transfer calculations based on these values and an

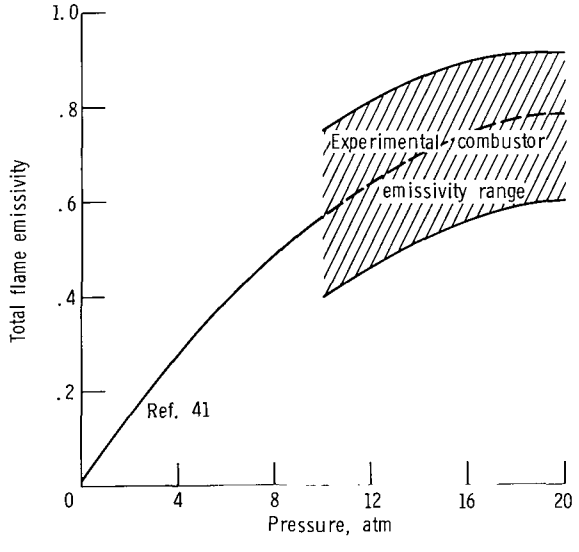

Figure 16. - Comparison of experimentally determined total emissivity with reference 41.

assumed burning rate to estimate flame temperature can be used to calculate realistic liner cooling requirements for widely different types of combustor configurations.

Effect of vitiation on observed flame temperature. - To obtain inlet temperatures higher than 589 K (1060° R) required that air be vitiated. Vitiation resulted in cold absorbing combustion products present in the primary combustion air. The primary air is admitted concentric to the fuel spray and hence envelopes the burning zone. When primary air containing the cold absorbing species intercepts the flame, radiation analysis becomes complex. A trend of erroneously low observed flame temperature would be expected from consideration of the manner in which the flame radiation is intercepted by the absorbing media. The flame temperature was calculated from the observed radiance at 2.7 micrometers, and adsorption in this region would result in too low a value for the flame temperature. Emissivity calculated under these conditions would be abnormally high.

About half of the experimental combustors investigated exhibited abnormal emissivities at 20 atmospheres pressure with vitiated air. No configuration exhibited this characteristic with indirectly heated inlet air even in cases for which a great deal of smoke was formed in the primary zone. The high concentration of smoke in the primary zone will lead to high emissivities and radiation similar to that of a blackbody radiator as reported in reference 14. An error in flame temperature assignment under these conditions, due to cool combustion products, would be readily noted. Therefore, it is concluded that indirectly heated inlet air must be used to avoid errors inherent in radiation measurements when vitiated air is used.

CONCLUDING REMARKS

The smoke particles formed during the combustion process will control to a large extent the radiation level to the primary zone combustor wall and the exhaust smoke number. From the preliminary results of this investigation, it is shown that smoke formation is largely controlled by the fuel and air introduction. At high combustor pressures, it becomes increasingly more important to provide and maintain a relatively lean primary zone. A lean primary zone in turn is detrimental to altitude relight capability. It is possible that a compromise between smoke and reliable relight characteristics may entail a greater degree of primary smoke formation than is desirable.

The lower practical limit of smoke formation at high pressure operation has not been established. The data of this report have shown that the oxidation process within the combustor is an important step in the reduction of the visible smoke. It is possible that, as the trend towards shorter combustors is continued, a reduction in primary zone length may result in an increase in exhaust smoke. The effect of residence time on the

oxidation rate of the carbon formed is included in equation (10); however, specific data are not available that show this effect in application to combustor design.

SUMMARY OF RESULTS

A technique was demonstrated that can be used to determine the smoke concentration within a combustor from the spectral radiance of the flame. Three combustor configurations incorporating features that improved the mixing of the primary fuel and air were operated at pressure levels of 10 and 20 atmospheres with inlet temperatures of 589 and 756 K (1060° and 1360° R) over a range of fuel-air ratios. Specific results are quoted for an operating condition of 20 atmospheres pressure, inlet temperature of 589 K (1060° R), reference velocity of 21.3 meters per second (70 ft/sec), and fuel air-ratio of 0.014. Smoke in the primary zone was determined from calculations based on the spectral emissivity of the luminous smoke particles and the exhaust smoke concentration was based on smoke number determinations from stained filter paper tape. It was shown that

1. A primary zone smoke concentration can be determined from the calculated spectral emissivity of the smoke.

2. Primary zone smoke concentration was of the order of 100 to 1000 times greater than observed at the exhaust. More than 99 percent of the smoke formed is burned within the combustion chamber before the exhaust.

3. The smoke oxidation rate was calculated from the difference in smoke concentration determined in the primary zone and at the combustor exhaust. A specific reaction rate of the order of 2.5×10^{-4} grams carbon per square centimeter per second was indicated. The rate was relatively independent of geometric configuration of the combustor.

4. The total radiance from the flame increased as the combustor pressure and fuel-air ratio increased.

5. A relationship was established from which the total flame radiation in the primary zone can be estimated from the exhaust smoke number. At the threshold of visible smoke (smoke number of 25) the total flame radiation level was 36.2 watts per square centimeter per steradian (113 670 Btu/(hr)(ft^2)(sr)).

6. Major improvements in lowering the total flame radiation are shown to be possible if the exhaust smoke is reduced below the visible threshold by means of primary combustor zone design. Approximately a threefold reduction in radiation level to the combustor liner was indicated by reducing the smoke number level from 32 to 4.

7. Smoke is the primary source of flame emissivity at high combustor pressures. The flame emissivity was 0.9, 0.6, and 0.75 for combustor models A, B, and C, re-

spectively, corresponding to flame temperatures of 2230, 2040, and 2200 K (4014°, 3672°, and 3960° R). The normal nonluminous emissivity of the combustion products was 0.27.

8. Significant changes in smoke emission levels can be obtained by designs that affect the mixing rate of fuel and air. A smoke number reduction from 32 to 4 was achieved by combustor design changes.

Lewis Research Center,
National Aeronautics and Space Administration,
Cleveland, Ohio, April 1, 1971,
720-03.

APPENDIX A

SYMBOLS

A	constant
c	mass concentration of radiating species (smoke in this study)
c_1	$2\pi c^2 h = 3.7413 \times 10^{-12}$ W-cm^2
c_2	hc/k = 1.4388 cm-deg
d	smoke particle diameter
E	activation energy
$K_{\lambda, T}$	extinction coefficient (Mie theory)
K_{λ}	absorption coefficient (Mie theory)
$K_{S, \lambda}$	scattering coefficient (Mie theory)
k	universal gas constant
$k_{\lambda, T}$	absorption coefficient (general)
k_1, k_2	reaction rate constants
L	radiance
ℓ	optical length
ℓ'	reaction zone length
$N_{(\lambda)}$	detector responsivity
N_{peak}	peak detector responsivity
p	pressure
R	specific reaction rate
R_L	specific reaction rate Langmuir isotherm model
R_s	reflectance measurement of smoke stained Whatman No. 4 filter paper
R_w	reflectance measurement of clean Whatman No. 4 filter paper
T	temperature
t	time
V_r	reference velocity, based on maximum cross section of combustor housing
α	absorptivity
δ	Stephan-Boltzmann constant
ϵ	emissivity
λ	wavelength
ρ	smoke density

Subscripts:

B	blackbody
T	temperature
λ	wavelength
0	initial
1	adsorption
2	desorption

APPENDIX B

EXPERIMENTAL COMBUSTORS

The combustor configurations were designed to produce a minimum of smoke formation and to reduce the combustor overall length as compared with conventional combustors.

Combustor design. - It has been shown that if the local equivalence ratio exceeds a value much greater than 1.5, a smoke threshold level will be reached and appreciable smoke will be formed particularly at pressure levels above 5 atmospheres as shown in reference 2. The reaction rate of the fuel and air at these pressures is also increased so that the combustion and the combustion byproducts are influenced primarily by the degree of mixing between the fuel and air. In the three combustor models almost all the primary air is brought into the inlet snout and distributed by means of swirlers in a concentric cone around the fuel nozzle to promote mixing.

Three variations of the primary zone are represented as shown in the schematic diagrams for combustor models A, B, and C (fig. 17(b)). Significant variations in the

TABLE IV. - PRIMARY COMBUSTION-ZONE DETAILS

Combustor model	Percent of air to swirlers	Type of fuel nozzle	Primary-zone hole pattern
A	24	Variable area (P = 10 atm) pintle type	None
B	34	Fixed area (P = 20 atm)	None
C	34	Fixed area (P = 20 atm)	Five holes on outer wall only (diam., 2.22 cm or 0.875 in.) equally spaced 6.67 cm (2.63 in.) from nozzles

details of the primary zone are shown in table IV. The condition where 34 percent of the area is open to the swirlers corresponds to the distribution of fuel and air required to reach stoichiometric at typical engine takeoff.

The secondary mixing zone consists of slots so placed that alternate jets of dilution gases from opposing walls are interleaved in order to promote rapid mixing as discussed in reference 32. Models A and B had identical dilution mixing sections. In model C,

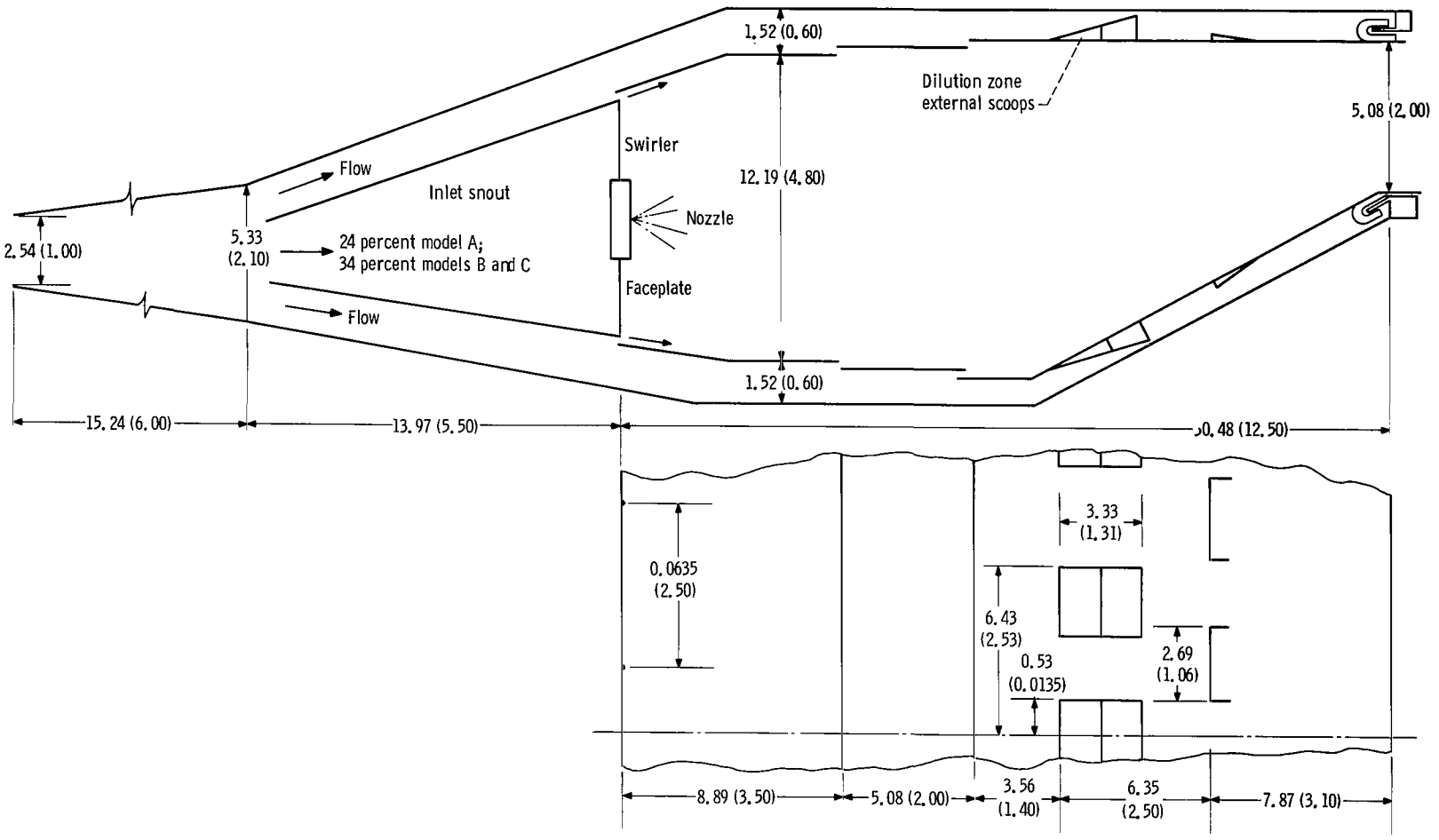

Figure 17. - Combustor configuration (all dimensions in cm (in.)).

the inner wall had alternate strips cut 0.64 centimeter (0.25 in.) wide between the main slots to improve the outlet temperature profile.

Combustor performance. - The combustor performance was determined from indications of pressure and temperature from rakes installed at the diffuser inlet (see fig. 17) and from indication of pressure and temperature from a probe which traversed the exhaust. The combustion efficiency was above 95 percent for the three combustor models, and the total pressure loss was of the order of 5 to 6 percent for a diffuser inlet Mach number of 0.28 (combustor reference velocity = 21.3 m/sec (70 ft/sec)). Combustor altitude relight capability was not investigated. Combustor blowout was encountered as the total inlet pressure was reduced to below/atmosphere for an inlet temperature of 589 K (1060° R) and a combustor reference velocity of 21.3 meters per second (70 ft/sec).

Additional combustor configurations. - Data obtained with six or seven additional combustor configurations are also included to evaluate trends of total radiance, smoke number, and specific reaction rates. These combustors featured different types of inlet air swirlers, inlet air splits (from 14 to 34 percent), different fuel nozzles, and changes in the dilution air mixing pattern. The pertinent radiation and smoke data in general fell between the extremes represented by combustor models A and B. Since complete experimental data were not obtained with all models tested, the data from these models are included for correlation purposes only.

APPENDIX C

ANALYSIS OF ASTM A-1 FUEL

The analysis was performed using U.S. Customary Units.

Specific gravity:	
At 78° F	45.1
At 60° F	43.6
At 60°/60° F	0.8081
Smoke point, min	24
Net heat of combustion, Btu/lbm	18 605
Aromatics, percent	12
Hydrogen to carbon ratio	0.160

REFERENCES

1. Thomas, A.: Carbon Formation in Flames. Combustion and Flames, vol. 6, Mar. 1962, pp. 46-62.

2. Macfarlane, J. J.; Holderness, F. H.; and Whitcher, F. S. E.: Soot Formation Rates in Premixed C_5 and C_6 Hydrocarbon-Air Flames at Pressures up to 20 Atmospheres. Combustion and Flame, vol. 8, Sept. 1964, pp. 215-229.

3. Toone, B.: A Review of Aero Engine Smoke Emission. Combustion in Advanced Gas Turbine Systems. I. E. Smith, ed., Pergamon Press, 1968, pp. 271-293.

4. Thring, M. W.; Foster, P. J.; McGrath, I. A.; and Ashton, J. S.: Prediction of the Emissivity of Hydrocarbon Flames. Internation Developments in Heat Transfer. ASME, 1963, pp. 796-803.

5. Godridge, A. M.; and Hammond, E. G.: Emissivity of a Very Large Residual Fuel Oil Flame. Twelfth Symposium (International) on Combustion. Combustion Institute, 1969, pp. 1219-1228.

6. Beer, J. M.; and Howarth, C. R.: Radiation from Flames in Furnaces. Twelfth Symposium (International) on Combustion. Combustion Institute, 1969, pp. 1205-1217.

7. Howarth, C. R.; Foster, P. J.; and Thring, M. W.: The Effect of Temperature on the Extinction of Radiation by Soot Particles. Proceedings of the Third Internation Heat Transfer Conference. Vol. 5. AIChE, 1966, pp. 122-128.

8. Stull, V. Robert; and Plass, Gilbert N.: Emissivity of Dispersed Carbon Particles. J. Opt. Soc. Am., vol. 50, no. 2, Feb. 1960, pp. 121-129.

9. Dalzell, W. H.; and Sarofim, A. F.: Optical Constants of Soot and Their Application to Heat-Flux Calculations. J. Heat Transfer, vol. 91, no. 1, Feb. 1969, pp. 100-104.

10. Foster, P. J.: Calculation of the Optical Properties of Dispersed Phases. Combustion and Flame, vol. 7, Sept. 1963, pp. 277-282.

11. Boynton, F. P.; Ludwig, C. B.; and Thomson, A.: Spectral Emissivity of Carbon Particle Clouds in Rocket Exhausts. AIAA J., vol. 6, no. 5, May 1968, pp. 865-871.

12. Gaydon, A. G.; and Wolfhard, H. G.: Flames, Their Structure, Radiation, and Temperature. Chapman & Hall, 1953.

13. Millikan, Roger C.: Sizes, Optical Properties, and Temperatures of Soot Particles. Temperature. Its Measurement and Control in Science and Industry. Vol. III, Part 2, Applied Methods and Instruments. A. I. Dahl, ed. Rienhold Publ. Co., 1962, pp. 497-507.

14. Schirmer, R. M.; McReynolds, L. A.; and Daley, J. A.: Radiation from Flames in Gas Turbine Combustors. SAE Trans., vol. 68, 1960, pp. 554-561.

15. Hornbeck, George A.; and Olsen, Lief O.: Emission and Absorption Studies of Jet Engine Hydrocarbon Combustion Products. National Bureau of Standards (WADC TR 57-516, DDC No. AD-203791), Oct. 1958.

16. Simmons, F. S.; Yamada, H. Y.; and Arnold, C. B.: Measurement of Temperature Profiles in Hot Gases by Emission-Absorption Spectroscopy. Rep. WRL-8962-18-F, Michigan Univ. (NASA CR-72491), Apr. 1969.

17. Butze, Helmut F.: Effect of Inlet-Air and Fuel Parameters on Smoking Characteristics of a Single Tubular Turbojet-Engine Combustor. NACA RM E52A18, 1952.

18. Shayeson, M. W.: Reduction of Jet Engine Exhaust Smoke With Fuel Additives. Paper 670866, SAE, 1967.

19. Essenhigh, R. H.; Froberg, R.; and Howard, J. B.: Combustion Behavior of Small Carbon Particles. Ind. Eng. Chem., vol. 57, no. 9, Sept. 1965, pp. 32-43

20. Tu, C. M.; Davis H.; and Hottel, H. C.: Combustion Rate of Carbon. Ind. Eng. Chem., vol. 26, no. 7, July 1934, pp. 749-757.

21. Gulbransen, Earl A.; and Andrew, Kenneth F.: Reactions of Artificial Graphite. Ind. Eng. Chem., vol. 44, no. 5, May 1952, pp. 1034-1047.

22. Smith, David F.; and Gudmundsen, Austin: Mechanism of Combustion of Individual Particles of Solid Fuels. Ind. Eng. Chem., vol. 23, no. 3, Mar. 1931, pp. 277-285.

23. Lee, K. B.; Thring, M. W.; and Beer, J. M.: On the Rate of Combustion of Soot in a Laminar Soot Flame. Combustion and Flame, vol. 6, Sept. 1962, pp. 137-145.

24. Fenimore, C. P.; and Jones, G. W.: Oxidation of Soot by Hydroxyl Radicals. J. Phys. Chem., vol. 71, no. 3, Feb. 1967, pp. 593-597.

25. Wiebelt, John A.: Engineering Radiation Heat Transfer. Holt, Rinehart and Winston, 1966.

26. Liebert, Curt H.; and Hibbard, Robert R.: Spectral Emittance of Soot. NASA TN D-5647, 1970.

27. Siddall, R. G.; and McGrath, I. A.: The Emissivity of Luminous Flames. Ninth Symposium (International) on Combustion. Academic Press, 1963, pp. 102-110.

28. Anon.: Aircraft Gas Turbine Exhaust Smoke Measurement. Aerospace Recommended Practice 1179, SAE, Apr. 1970.

29. Shaffernocker, Wayne M.; and Stanforth, Charles M.: Smoke Measurement Techniques. Paper 680346, SAE, Apr. 1968.

30. Shertler, Ronald J.; and Norgren, Carl T.: Experimental Investigation of Charging Submicron Carbon Powder for Colloidal Particle Thrustors. NASA TN D-3657, 1966.

31. Roudebush, William H.: State of the Art in Short Combustors. Presented at the Sixth Congress of the International Council of the Aeronautical Sciences, Munich, Germany, Sept. 9-13, 1968.

32. Norgren, Carl T.; and Humenik, Francis M.: Dilution-Jet Mixing Study for Gas-Turbine Combustors. NASA TN D-4695, 1968.

33. Metzler, Allen J.; and Branstetter, J. Robert: Fast Response, Blackbody Furnace for Temperatures up to 3000° K. Rev. Sci. Inst., vol. 34, no. 11, Nov. 1963, pp. 1216-1218.

34. Vizzini, Russell W.: Problems Encountered During the Development of Smokeless Gas Turbine Engines for Naval Aircraft. Rep. NAPTC-ATD-174, Naval Air Propulsion Test Center, Aug. 1969. (Available from DDC as AD-860562L.)

35. Bagnetto, Lucien: Smoke Abatement in Gas Turbine. Part 2: Effects of Fuels, Additives and Operating Conditions on Smoke Emissions and Flame Radiation. Rep. 5127-68-Pt. 2, Phillips Petroleum Co., Sept. 1968. (Available from DDC as AD-842818.)

36. Schirmer, R. M.; and Quigg, H. T.: High Pressure Combustor Studies of Flame Radiation as Related to Hydrocarbon Structure. Rep. 3952-65R, Phillips Petroleum Co., May 20, 1965. (Available from DDC as AD-617191.)

37. Linden, Lawerence H.; and Heywood, John B.: Smoke Emission From Jet Engines. Publ. 70-12, Fluid Mechanics Lab., Massachusetts Inst. Tech., Oct. 1970.

38. Essenhigh, R. H.; and Kurylko, L.: The Unsteady and Steady Combustion of Carbon. Rep. FS69-2(U), Pennsylvania State Univ., June 1969. (Available from DDC as AD-699531.)

39. Golovina, E. S.; and Khaustovich, G. P.: The Interaction of Carbon with Carbon Dioxide and Oxygen at Temperatures up to 3000° K. Eighth Symposium (International) on Combustion. Williams & Wilkins Co., 1962, pp. 784-792.

40. McAdams, William H.: Heat Transmission. Third ed., McGraw-Hill Book Co., Inc., 1954.

41. Clarke, J. S.; and Jackson, S. R.: General Considerations in the Design of Combustion Chambers for Aircraft and Industrial Gas Turbines. Presented at the International Congress and Exposition of Automotive Engineering, SAE, Detroit, Mich., 1962.

NASA-Langley, 1971 —— 33 E-6083

013 001 C1 U 33 710716 S00903DS
DEPT OF THE AIR FORCE
WEAPONS LABORATORY /WLOL/
ATTN: E LOU BOWMAN, CHIEF TECH LIBRARY
KIRTLAND AFB NM 87117

"The aeronautical and space activities of the United States shall be conducted so as to contribute . . . to the expansion of human knowledge of phenomena in the atmosphere and space. The Administration shall provide for the widest practicable and appropriate dissemination of information concerning its activities and the results thereof."

—NATIONAL AERONAUTICS AND SPACE ACT OF 1958

NASA SCIENTIFIC AND TECHNICAL PUBLICATIONS

TECHNICAL REPORTS: Scientific and technical information considered important, complete, and a lasting contribution to existing knowledge.

TECHNICAL NOTES: Information less broad in scope but nevertheless of importance as a contribution to existing knowledge.

TECHNICAL MEMORANDUMS: Information receiving limited distribution because of preliminary data, security classification, or other reasons.

CONTRACTOR REPORTS: Scientific and technical information generated under a NASA contract or grant and considered an important contribution to existing knowledge.

TECHNICAL TRANSLATIONS: Information published in a foreign language considered to merit NASA distribution in English.

SPECIAL PUBLICATIONS: Information derived from or of value to NASA activities. Publications include conference proceedings, monographs, data compilations, handbooks, sourcebooks, and special bibliographies.

TECHNOLOGY UTILIZATION PUBLICATIONS: Information on technology used by NASA that may be of particular interest in commercial and other non-aerospace applications. Publications include Tech Briefs, Technology Utilization Reports and Technology Surveys.

Details on the availability of these publications may be obtained from:

SCIENTIFIC AND TECHNICAL INFORMATION OFFICE

NATIONAL AERONAUTICS AND SPACE ADMINISTRATION

Washington, D.C. 20546